

State of the art report on the use of press-in piling data for estimating subsurface information

Y. Ishihara
Giken, Kochi, Japan

O. Kusakabe
International Press-in Association, Tokyo, Japan

ABSTRACT: The construction and design of structures with piles are usually conducted based on limited number of results of subsurface investigations, which will be conducted typically at the intervals of several tens or one hundred meters. On the other hand, there are local variations in the actual ground, which could exist in a smaller area than the spatial intervals of the subsurface investigations. As a result, the prior information and the actual condition of the ground can be different, which deteriorates the rationality of the construction and design. The press-in piling data obtained for every single pile are expected to provide an effective solution, by being applied to the automatic machine operation or to the estimation of the subsurface information. This paper introduces the methods of estimating the subsurface information from press-in piling data, most of which were organized into a technical material in Japanese under the activity of IPA-TC2.

1 INTRODUCTION

1.1 Outline of the Press-in Method

The Press-in Method is one of the piling methods. As it installs piles using a static jacking force, it generates less noise and vibration. It gains a reaction force by firmly grasping the previously installed piles, and thus saves temporary works as shown in Figure 1 and reduces the possibility of roll-over accidents. In addition, as it grasps piles not at the pile head but near the ground surface, it requires less headroom as shown in Figure 2.

There are four penetration techniques in the Press-in Method, as summarized in Figure 3. The basic one is “Standard Press-in” where no installation assistance such as water jets or augers are used. It is noted that “surging”, a repeated penetration and extraction during installation, is not taken as an installation assistance and can be adopted in any of the four penetration techniques. The other three are “Press-in with Water Jetting” where water jets are used in the pile base, “Press-in with Augering” where soils near the pile base are excavated and temporarily lifted up, and “Rotary Cutting

Press-in” where piles with base cutting teeth are pushed and rotated at the same time. With the development of the latter two techniques, the applicability of the Press-in Method has been expanded to hard grounds including rocks and concretes.

More detailed information on the Press-in Method and its applications can be found in IPA (2016), IPA (2020) and Bolton *et al.* (2020).



Figure 1. Press-in piling system saving temporary works (JPA, 2017).



Figure 2. Press-in piling under a restriction of headroom (IPA, 2015).

1.2 Use of piling data in the Press-in Method

Generally, the construction and design of structures with piles are based on the subsurface information obtained by interpolating the limited number of

subsurface investigation results. The spatial intervals between two adjacent points of subsurface investigations are typically several tens or one hundred meters. On the other hand, it is often the case that local variations can be seen in the actual ground. For examples, the geological structure may not be homogeneous horizontally, and weak soils or hard cobbles may exist locally. If the areas of such local variations are smaller than the spatial intervals of the subsurface investigation points, the prior information and the actual condition of the ground becomes different. This difference deteriorates the rationality of the construction and design.

In the Press-in Method, piling data can be obtained for every single pile. This feature is expected to be utilized as ICT (Information and Communication Technology) to provide a solution for the above-mentioned issue.

The press-in piling data includes the jacking force, torque, penetration depth, time, rotational number and so on. As shown in Figure 4, applications of the data are exemplified by the selection of press-in conditions, the estimation of subsurface information and the estimation of the pile performance.

In the selection of press-in conditions, the values for the press-in parameters such as the downward velocity, upward velocity, downward displacement, upward displacement and so on, are selected based on a judgement using the piling data. A good example is the automatic operation system where the press-in conditions selected based on the piling data





Standard Press-in	Press-in with Water Jetting	Press-in with Augering	Rotary Cutting Press-in
			
Press-in a pile without installation assistance	Press-in a pile while applying water-jetting in the pile base	Press-in a pile while excavating the soil around the pile base	Rotate and press-in a pile equipped with base cutting teeth

Figure 3. Four penetration techniques in the Press-in Method.

are feed-backed to the press-in machine continuously during the piling work (Ishihara, 2018).

The estimation of the subsurface information is to estimate the information (type and state) of the soil around the pile base, by interpreting the piling data. The estimated information would realize a more reliable termination control management (construction management at the end of installation of each pile), or provide contractors with objective materials for judging the necessity of changing the penetration techniques or the pile embedment depth.

The estimation of the pile performance means estimating the performance (such as the vertical capacity and the horizontal resistance) of the installed piles from the piling data. Although the confirmation of the pile performance is usually done by the load tests, they cannot be conducted for all the piles because of the additional time and cost required for them. If the pile performance is estimated from the piling data, it would become possible to assure a certain level of quality for all the piles without causing the issue of additional time and cost.

1.3 Objectives of this paper

Among the four applications of the piling data explained in the previous section, this paper introduces the methods of estimating the subsurface information, by re-structuring and adding recent findings to the contents in the IPA-TC2 technical material written in Japanese (IPA, 2017).

The penetration techniques dealt with in this paper will be Standard Press-in, Press-in with Augering and Rotary Cutting Press-in. For Standard Press-in, methods of estimating the cone resistance (q_c) of CPT (Cone Penetration Test), soil type and N value of SPT (Standard Penetration Test) will be discussed. For the other two penetration techniques, methods of estimating the SPT N value will be discussed.

In the hard ground, the SPT N values often exceeds 50 (more precisely, the SPT sampler does not penetrate into the virgin ground by the

designated value of 0.3 meters even when the blow count reaches 50). In such cases, this paper will adopt the converted N value as expressed by:

$$\text{Converted } N = 50 \times \frac{0.3 \text{ [m]}}{\delta z_{\text{SPT}(50)} \text{ [m]}} \quad (1)$$

where $\delta z_{\text{SPT}(50)}$ is the incremental penetration depth of the SPT sampler for the blow count of 50 (JGS, 2015).

There are several examples of the use of piling data in other piling methods. For bored piles or driven piles (using vibratory hammers), methods of confirming the bearing stratum based on the electric current values required for operating augers or vibratory hammers (Hashizume *et al.*, 2002; JRA, 2015; JFCC & COPITA, 2017). For driven piles, methods of estimating a static vertical capacity of a pile based on the piling data obtained by using an instrumented pile (Likins, 1984; Rausche *et al.*, 1985) are widely known. On the other hand, the methods in this paper are different from the above-mentioned existing methods in that they are based on the static loads during the piling work, which would allow simpler interpretation of the data, and that they do not require complicated instrumentation with piles (other than a device for measuring the length of the soil inside the pile, as explained in Section 4).

2 ESTIMATION FROM PILING DATA OBTAINED IN STANDARD PRESS-IN

In Standard Press-in, a pile is installed by a static jacking force without the use of any installation assistance, and the process of the penetration of the pile is similar to that of a cone in CPT. This similarity has been taken into account to estimate the subsurface information from the piling data in Standard Press-in (Ishihara *et al.*, 2015a). The outline of the flow of estimation is shown in Figure 5.

2.1 Estimating base resistance and shaft resistance

The load applied to the pile head (head load, Q) is the sum of the resistance on the pile base (base resistance, Q_b) and the resistance on the pile shaft (shaft resistance, Q_s). To estimate the subsurface information at the pile base, it is better to use Q_b rather than Q , as Q_b reflects the information of the soil beneath the pile base more directly. To obtain Q_b without any instrumentation on piles, a method using the data of press-in with surging has been confirmed to be effective.

In press-in with surging, the downward displacement (l_d) and upward displacement (l_u) are applied to the pile alternately ($l_d > l_u$), as shown in Figure 6. Ogawa *et al.* (2012) conjectured that, as shown in Figure 7, the head load recorded when the pile base passes a certain depth for the first time (Q_1) is the sum of Q_b and Q_s , while the head load recorded

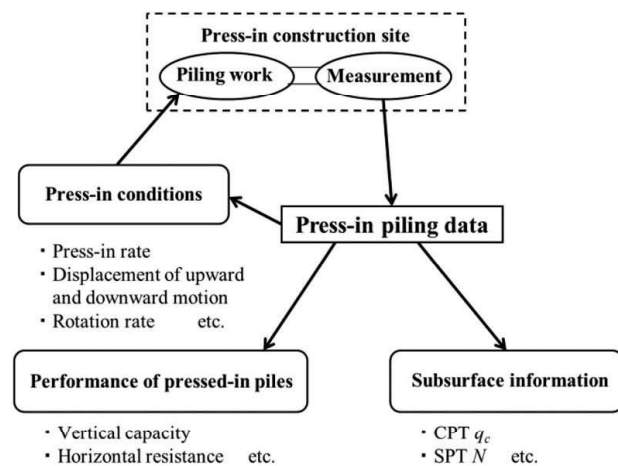


Figure 4. Use of piling data in the Press-in Method.

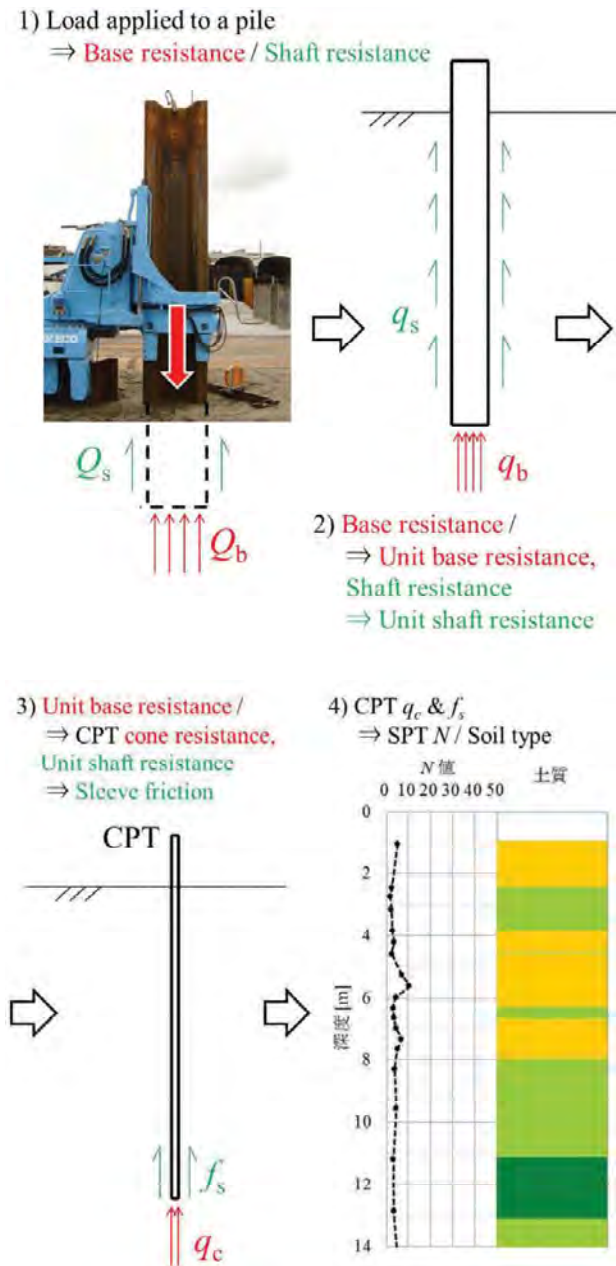


Figure 5. Flow of estimation in Standard Press-in.

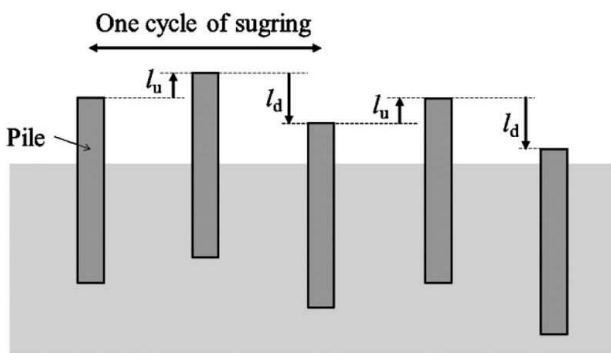


Figure 6. Process of surging.

when the pile base passes that depth for the second time (Q_2) consists only of Q_s , as expressed by the following two equations.

$$Q_1 = Q_b + Q_s \quad (2)$$

$$Q_2 = Q_s \quad (3)$$

From these equations, Q_b can be expressed as:

$$Q_b = Q_1 - Q_2 \quad (4)$$

They argued that the values of Q_1 and Q_2 should be obtained shortly after the beginning of the downward motion in each cycle of surging, in order to avoid the influence of soils that may have collapsed into the void created beneath the pile base during the previous upward motion. Figure 8 shows the variation of Q and Q_s in one cycle of surging, which was obtained in C11 test series in a soft alluvial ground shown in Figure 9 by using a closed-ended pile with the outer diameter of 318.5 mm. The pile was equipped with a load cell in its base to measure Q_b , and Q_s was obtained by subtracting Q_b from Q . As can be confirmed in the figure, values of Q_s were similar in the first and the second penetrations. On the other hand, values of Q in the second penetration were identical with Q_s values when the downward displacement (increment in the penetration depth) in the second penetration was smaller than 0.1 m but gradually increased afterwards. Ishihara *et al.* (2015a) further analyzed the data obtained in C11 test series (C11-05) and confirmed that the difference between the estimated and measured Q_b values became larger with the increase in the second downward displacement (l_{d2}), regardless of the soil type or the penetration depth, as shown in Figure 10. Based on these, it is recommended to define the values of Q_1 and Q_2 as the arithmetic average of the Q values recorded in $0.1 D_o < l_{d2} < 0.2 D_o$, where D_o is the outer diameter of the pile.

Figure 11 Shows the comparison of Q_b measured by the load cell and Q_b estimated by Equation (4) in two tests in the C11 test series (C11-05 and C11-06). The two tests were conducted with the same condition ($l_d = 800\text{mm}$, $l_u = 400\text{mm}$) at different positions which were distant from each other by about 4 meters. Good agreement can be confirmed between the estimated and measured values in the depth

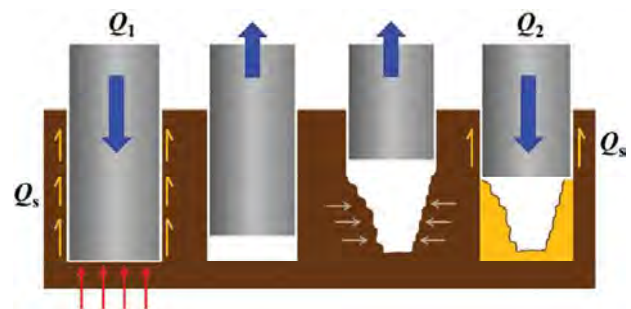


Figure 7. Forces acting on a pile during surging.

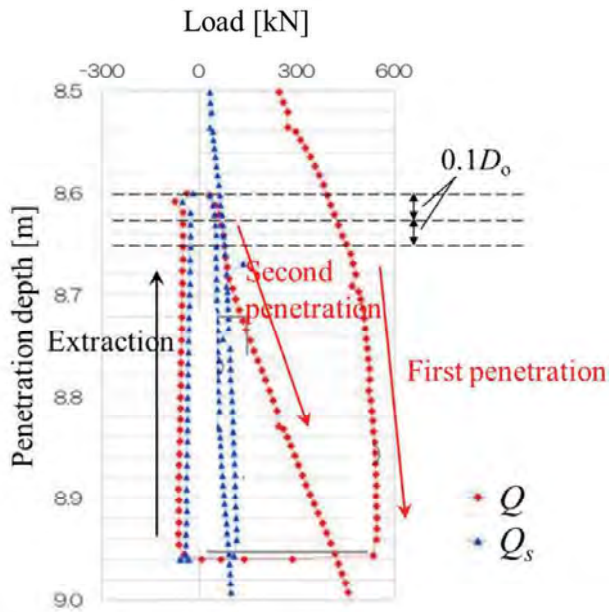


Figure 8. Variation of Q and Q_s in one cycle of surging.

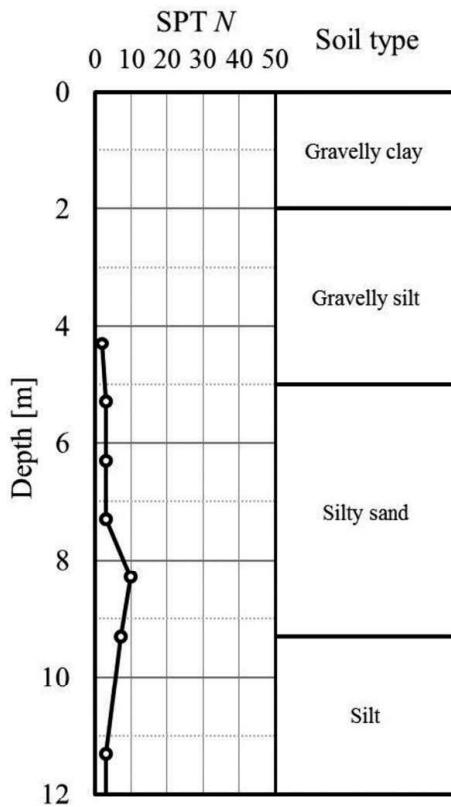
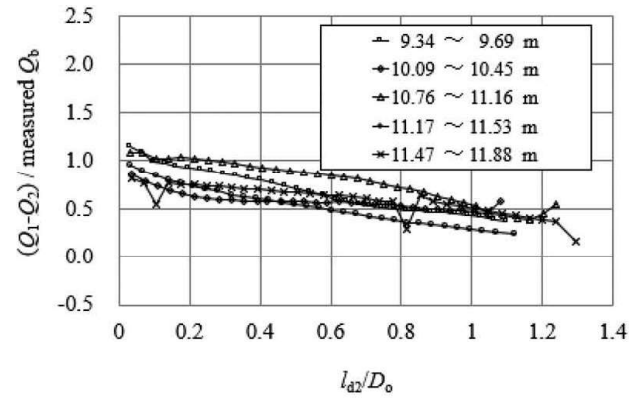


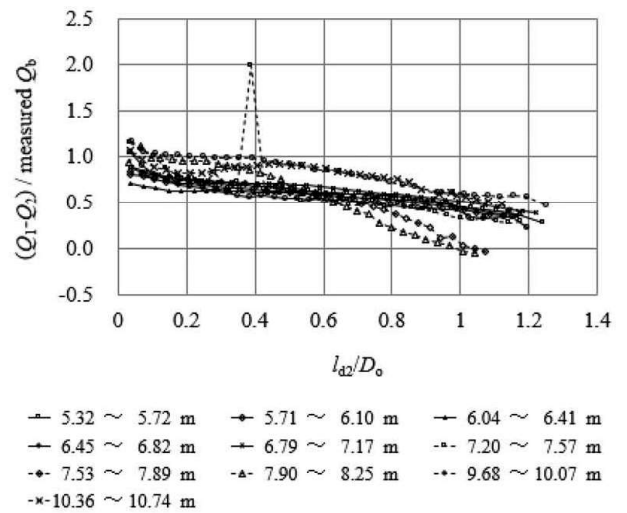
Figure 9. Site profiles of C11 test series.

range where N values show local peak values. On the other hand, in the depth range where N values are small, a trend of underestimation is confirmed. This underestimation might have been partly because the soil around the pile base was very weak and easily deformed toward the void beneath the pile base during the upward motion of the pile, leading to the increase in the Q_2 values.

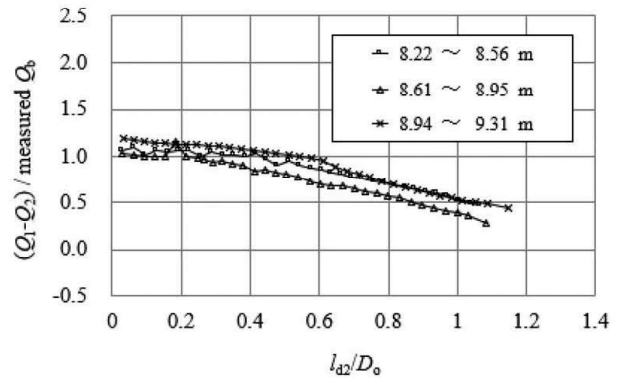
By the way, according to Ogawa *et al.* (2011), it is not a better option to assume the extraction force in each cycle of surging as being identical with Q_s . This seems to be partly due to the difference in $Q_b - Q_s$ interaction during the penetration and the extraction.



(a) In clay to silty clay



(b) In silty sand to sandy silt



(c) In sandy silt to clean sand

Figure 10. The ratio of estimated $Q_b (= Q_1 - Q_2)$ to measured Q_b plotted against l_{A2}/D_0 in each cycle of surging.

2.2 Estimating unit base resistance and unit shaft resistance

This sub-section discusses the method to estimate the unit base resistance (q_b) and the unit shaft resistance (q_s) from Q_b and Q_s .

2.2.1 Estimating unit base resistance of open-ended tubular piles

Regarding the pile base, it is necessary to consider the plugging condition. For open-ended tubular piles, it is possible to assess the plugging condition based on the index called *IFR* (Incremental Filling Ratio) as expressed by the following equation (White & Deeks, 2007; Lehane *et al.*, 2007; White *et al.*, 2010).

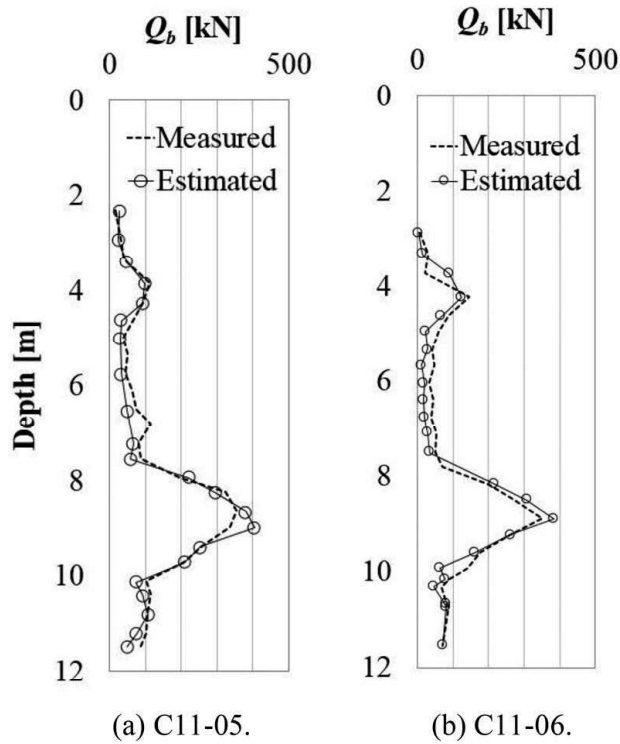


Figure 11. Comparison of estimated and measured Q_b (Closed-ended, $D_o = 318.5\text{mm}$).

$$IFR = \frac{\delta h}{\delta z} \quad (5)$$

Here, δz is the increment of the penetration depth, and δh is the increment of the length of the soil column inside the pile that is observed while the penetration depth increases by δz . The fully plugged condition, the fully unplugged condition and the partially plugged condition are represented by $IFR = 0$, $IFR = 1$ and $0 < IFR < 1$ respectively.

For open-ended tubular piles, Q_b is expressed as the sum of the resistance on the bottom of the inner

soil column (Q_{bi}) and the resistance on the pile base annulus (Q_{bp}):

$$Q_b = Q_{bi} + Q_{bp} \quad (6)$$

Q_{bp} could be assumed as:

$$Q_{bp} = \left(\frac{\pi D_o^2}{4} - \frac{\pi D_i^2}{4} \right) \times q_{b,closed} \quad (7)$$

where $q_{b,closed}$ is the unit base resistance of a closed-ended pile, and D_o and D_i are the outer and inner diameter of the pile respectively. On the other hand, the inner soil column receives not only Q_{bi} but also its self-weight (W_s) and the inner shaft resistance (Q_{si}) as shown in Figure 12, and these forces will satisfy the following equilibrium condition:

$$Q_{bi} = W_s + Q_{si} \quad (8)$$

Kurashina (2016) conducted model tests to press-in a closed-ended pile ($D_o = 101.6\text{mm}$) or an open-ended pile ($D_o = 101.6\text{mm}$, $D_i = 83.5\text{mm}$) in a dry sand with the relative density being around 60%. The closed-ended pile was equipped with strain gauges in its base to measure Q_b , while the open-ended pile was equipped with a load cell in its head to measure Q_{bi} and a stroke sensor to obtain the length of the inner soil column, as shown in Figure 13. Figure 14 shows the correlation of $(1 - IFR)$ and the right side of Equation (8) normalized by the potential push-up stress at the bottom of the inner soil column ($= (\pi D_i^2/4) q_{b,closed}$), which were obtained by analyzing the data of Kurashina (2016). Based on this figure, the following correlation is found:

$$\frac{W_s + Q_{si}}{\frac{\pi D_i^2}{4} \times q_{b,closed}} = \lambda \times (1 - IFR) \quad (9)$$

which is basically in line with the findings of Lehane & Gavin (2001). This equation is converted into:

$$W_s + Q_{si} = \lambda \times (1 - IFR) \times \frac{\pi D_i^2}{4} \times q_{b,closed} \quad (10)$$

Combining Equations (8) and (10),

$$Q_{bi} = \frac{\pi D_i^2}{4} \times \lambda \times (1 - IFR) \times q_{b,closed} \quad (11)$$

The value of λ is difficult to be reliably determined, because the number of the database is limited. Tentatively, it will be assumed as unity (smaller than the experimental results), which will give a conservative estimation results (smaller SPT N values and soil types with smaller grain sizes) based on the methods explained later. Combining Equations (6), (7) and (11),

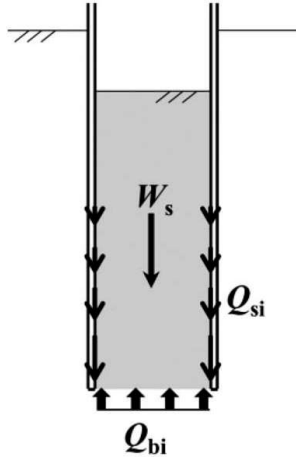


Figure 12. Forces acting on the soil column inside the pile.

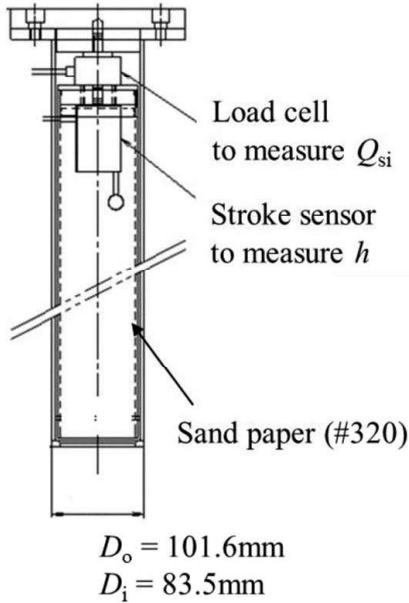


Figure 13. Open-ended model pile to measure Q_{si} .

$$q_{b,closed} = \frac{Q_b}{\frac{\pi D_o^2}{4} - IFR \times \frac{\pi D_i^2}{4}} \equiv \frac{Q_b}{A_{b,eff}} \quad (12)$$

where $A_{b,eff}$ is the effective base area reflecting the plugging condition.

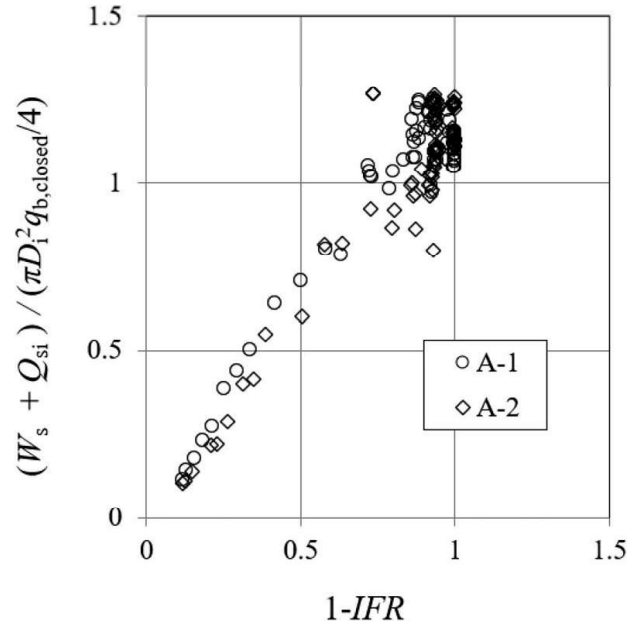


Figure 14. Correlation between $\frac{W_s + Q_{si}}{\frac{\pi D_i^2}{4} \times q_{b,closed}}$ and $(1-IFR)$.

2.2.2 Estimating unit base resistance of sheet piles

For sheet piles, phenomena similar to the plugging of tubular piles have been empirically known by contractors. The increase in the density of the soil around the base of the sheet pile was confirmed in model tests by Taenaka *et al.* (2006) using X-ray. In this paper, to consider the plugging condition for sheet piles, the complicated shape of sheet piles will be simplified by assuming an equivalent tubular pile that has the same sectional area both on the pile annulus and in the hollow part inside the pile as those of sheet piles, as shown in Figure 15. Example of the equivalent values of the sectional area of the pile base annulus ($A_{bp,eq}$), the sectional area inside the pile ($A_{bi,eq}$), the outer diameter ($D_{o,eq}$) and the inner diameter ($D_{i,eq}$) of several types of sheet piles are shown in Table 1.

However, it is not easy to measure the height of the surface of the soil in the hollow part of the sheet pile (to obtain the values of h) during the actual piling work. To cope with this difficulty, a constant plugging condition (i.e. the value of IFR) will be assumed for each type of sheet pile. Considering that the subsurface information estimated from the piling data will be more likely to be utilized for grasping the relatively hard layers, it will provide a practically reasonable IFR values if they are back-analyzed so that the local peak values of the N values estimated from the piling data match with the local peak values of the N values obtained by SPT. Table 2 shows the back-analyzed IFR values for three types of sheet piles.

Taenaka (2013) conducted a centrifuge model tests with the centrifugal acceleration being 20g, in which sheet piles were jacked into a dry sand. The height of the surface of the soil in the hollow part of the sheet pile was measuring by a steel bar, and the component of the surrounding soil collapsing into the hollow part was compensated by assuming an active failure. As a result, IFR was expressed as:

$$IFR = \min \left\{ 1.0, 1.12 \times \left(\eta_{sh} \times \frac{L}{W_b} \right)^{-0.45} \right\} \quad (13)$$

$$\eta_{sh} = \frac{\frac{1-\sin\theta}{\cos\theta} - \frac{W_b}{2 \times D_s} \times \left(\frac{\tau_b}{\tau_{si}} - 1 \right)}{1 - \frac{D_s}{W_b} \times \tan\theta} \quad (14)$$

where η_{sh} is the Arching Strength Parameter (a parameter depending on the shape of the sheet pile), L is the penetration depth, W_b , D_s and θ are the parameters related to the shape (length or angle) of the sheet pile as shown in Figure 16, and τ_b and τ_{si} are the frictional stress at the soil-soil or soil-pile interfaces.

The frictional force at the soil-soil interface (acting reversely to the direction of penetration) is generated in reaction to the frictional force at the soil-pile interface. It will follow that the former does not exceed the latter, leading to:

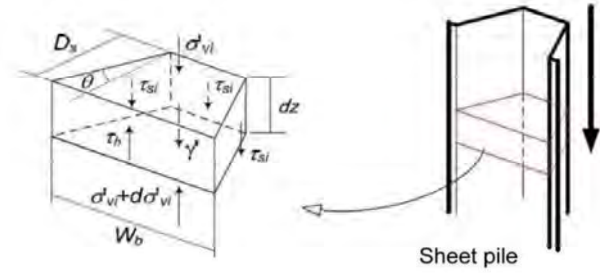


Figure 16. Explanation of symbols in Eqs. (13) and (14) (Taenaka, 2013).

$$\frac{\tau_b}{\tau_{si}} = \min \left\{ \frac{\tan\phi}{\tan\delta}, 1 - 2 \times \frac{D_s}{W_b} \times \left(\frac{1}{\cos\theta} - \tan\theta \right) \right\} \quad (15)$$

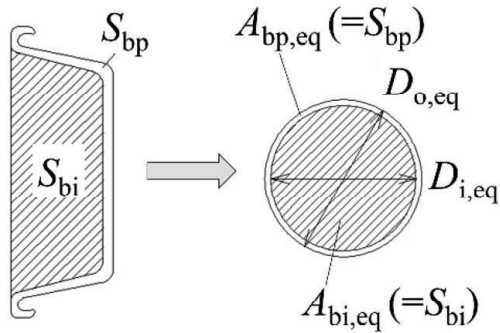


Figure 15. Conversion of a sheet pile into a tubular pile.

Table 1. Example of $A_{bp,eq}$, $A_{bi,eq}$, $D_{o,eq}$ and $D_{i,eq}$ of sheet piles.

Type of sheet piles	$A_{bp,eq}$ [m ²]	$A_{bi,eq}$ [m ²]	$D_{o,eq}$ [m]	$D_{i,eq}$ [m]
SP-III	0.0076	0.0435	0.2552	0.2353
SP-IIIw	0.0104	0.0910	0.3593	0.3403
SP-10H	0.0110	0.1068	0.3873	0.3688

Table 2. Back-analyzed IFR values for sheet piles.

Type of sheet piles	IFR
SP-III	0.50
SP-IIIw	0.90
SP-10H	0.95

Figure 17 shows the variation of IFR with depth for the three types of sheet piles, which were calculated by Equations (13), (14) and (15). Looking at the depth of 0.8 m, the IFR values for SP-10H, SP-IIIw and SP-III were 0.95, 0.81 and 0.60 respectively, which roughly corresponds to the values shown in Table 2 and suggests the validity of the back-analysis. However, considering that the IFR values sharply decreases with depth as can be seen in Figure 17, the IFR values in Table 2 might only be valid at a certain small penetration depth into a new layer.

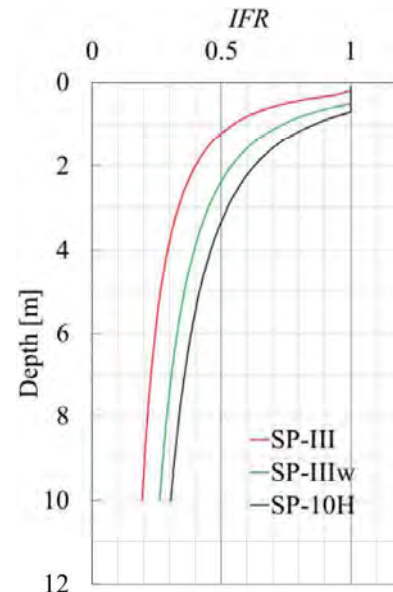


Figure 17. IFR values calculated by Eqs. (13) – (15).

2.2.3 Estimating unit shaft resistance of tubular piles or sheet piles

The unit shaft resistance will be obtained by:

$$q_s = \frac{Q_s}{A_{s,emb}} \quad (16)$$

where $A_{s,emb}$ is the area of the outer surface of the embedded part of the pile, as expressed by:

$$A_{s,emb} = \begin{cases} \pi \times D_o \times z_{emb} & (\text{for tubular piles}) \\ L_p \times z_{emb} & (\text{for sheet piles}) \end{cases} \quad (17)$$

where L_p is the perimeter of the sheet pile and z_{emb} is the embedment depth of the tubular pile or sheet pile.

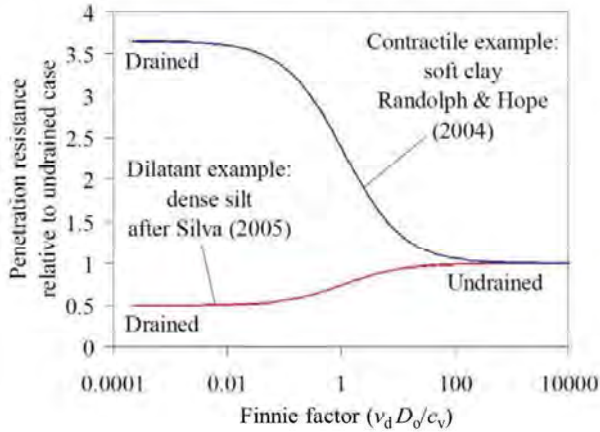


Figure 18. Expression of the rate effect by Finnie factor (after White *et al.*, 2010).

The unit shaft resistance q_s obtained by these equations is the average over the whole embedment depth. On the other hand, the sleeve friction (f_s) obtained in CPT, into which q_s is to be converted based on the method explained in the next sub-section, is the local frictional stress near the cone. Considering that the local frictional stress on the pile shaft will be higher near the pile base than far above the pile base, the average unit shaft resistance (q_s) will be smaller than the local unit shaft resistance near the pile base. As a result, the subsurface information estimated by using q_s (instead of the local unit shaft resistance near the pile base) becomes conservative (the estimated SPT N values will be smaller and the particle size of the estimated soil type will be smaller).

2.3 Estimating CPT cone resistance and sleeve friction

The next step is to convert $q_{b,closed}$ and q_s into CPT q_c and f_s . The CPT cone has much smaller diameter and is installed at a lower penetration rate than the pile. These differences will lead to differences in the resistance on the base and the shaft of the penetrating materials (i.e. the CPT cone or the pile). Therefore, the conversion of $q_{b,closed}$ and q_s into CPT q_c and f_s requires the consideration of the effects of the penetration rate and the scale (diameter of the penetrating material).

2.3.1 Effect of penetration rate

As an index to capture the rate effect on $q_{b,closed}$, a dimensionless quantity ‘‘Finnie factor’’ $v_d D_o / c_v$, where v_d is the downward velocity and c_v is the coefficient of consolidation, is widely known (Finnie & Randolph, 1994; White *et al.*, 2010). Figure 18 shows the example of explaining the rate effect by Finnie factor (White *et al.*, 2010). Based on this framework, the rate effect can be ignored if v_d is controlled to give the same value of Finnie factor during installation as that of CPT.

The rate effect on q_s seems to have not been well understood. In this paper, the approach using Finnie factor is assumed to be applicable to q_s as well as to $q_{b,closed}$. This is expected to be acceptable, as q_s can be expressed as a function of $q_{b,closed}$ according to Jackson *et al.* (2008) and Ishihara *et al.* (2011).

2.3.2 Effect of scale (pile diameter)

To consider the scale effect on $q_{b,closed}$, the knowledge on the scale effect on the unit base capacity ($q_{bf,closed}$) will be referred to, by assuming $q_{b,closed} = q_{bf,closed}$. Generally, the set-up phenomenon (the increase in the resistance with time after the end of installation) is mainly seen in the shaft resistance (Komurka *et al.*, 2003). It will follow that the effect of time after the end of installation on $q_{b,closed}$ could be ignored. Therefore, if the rate effect on $q_{b,closed}$ is ignored and the displacement to define $q_{bf,closed}$ is adequately chosen, the assumption of $q_{b,closed} = q_{bf,closed}$ would be acceptable.

It is known that $q_{bf,closed}$ becomes smaller as the outer diameter of the pile increases (Meyerhof, 1983; Jardine & Chow, 1996; Chow, 1997). In these researches $q_{bf,closed}$ is defined at a smaller displacement than what would give the ‘‘plunging load’’ (the load at a sufficiently large displacement, which reflects the fully mobilized strength of soils around the pile base). White & Bolton (2005) analyzed the database of Chow (1997) by defining $q_{bf,closed}$ by the plunging load, and confirmed that $q_{bf,closed}$ is not influenced by the pile diameter and can be linked with the averaged CPT cone resistance (q_{ca}) as:

$$q_{bf,closed} = \alpha \times q_{ca} \quad (18)$$

$$\alpha = 0.9 \quad (19)$$

As the base resistance during installation is mobilized in the process of the continuous penetration with a large displacement, it will be more appropriate to assume that $q_{b,\text{closed}}$ is comparable with the base capacity defined by the plunging load rather than the base capacity defined at a certain pile displacement. Then Equation (18) is re-written as:

$$q_{b,\text{closed}} = \alpha \times q_{ca} \quad (20)$$

On the other hand, the scale effect on q_s seems to have not been well understood. Based on the linear correlation between $q_{b,\text{closed}}$ and q_s , the scale effect on $q_{b,\text{closed}}$ (Eq. 20) will be assumed to be applicable to q_s as well, as expressed by:

$$q_s = \beta \times f_s \quad (21)$$

$$\beta = 0.9 \quad (22)$$

Ishihara *et al.* (2015) analyzed the piling data ($q_{b,\text{closed}}$ and q_s) obtained in a soft alluvial soil by using a closed-ended pile with $D_o = 318.5$ mm and the CPT results obtained in the same site. The back-analyzed values of α and β were 0.8 and 0.5 respectively, which are lower than the values shown in Equations (19) and (22). These lower values were possibly caused by the highly multilayered soil strata. Adopting Equations (19) and (22) will make the estimation results more conservative (the estimated SPT N values will be smaller and the particle size of the estimated soil type will be smaller).

2.4 Estimating SPT N and soil type

According to Robertson (1990), a value of an index I_c (Soil Behavior Type Index) is obtained from CPT q_c and f_s by:

$$I_c = \sqrt{(3.47 - \log Q_t)^2 + (1.22 + \log F_r)^2} \quad (23)$$

$$Q_t = \frac{q_c - \sigma_{v0}}{\sigma_{v0}'} \quad (24)$$

$$F_r = 100 \times \frac{f_s}{q_c - \sigma_{v0}} \quad (25)$$

where σ_{v0} and σ_{v0}' are the overburden pressure and the effective overburden pressure respectively. The soil type can then be obtained based on the I_c value and the chart shown in Table 3. On the other hand,

according to Jefferies & Davies (1993), SPT N can be estimated from CPT q_c and f_s by:

$$N = \frac{q_c}{8.5 \times \left(1 - \frac{I_c}{4.6}\right)} \quad (26)$$

where p_a is the atmospheric pressure (= 100 kPa).

Table 3. I_c values and soil types (Lunne *et al.* (1997)).

I_c	Soil type
$I_c < 1.31$	Gravelly sand
$1.31 < I_c < 2.05$	Sands - clean sand to silty sand
$2.05 < I_c < 2.60$	Sand mixtures - silty sand to sandy silt
$2.60 < I_c < 2.95$	Silt mixtures - clayey silt to silty clay
$2.95 < I_c < 3.60$	Clays
$3.60 < I_c$	Organic soils - peats

It is noted that it would be better to use the corrected cone resistance q_b , which compensates for the influence of pore water pressure on q_c , in the above equations. However, for simplicity, q_c will be consistently used in this paper. For soils other than soft fine soils, q_c and q_t can be taken as being comparable, according to Lunne *et al.* (1997). For soft fine soils, the excess pore water pressure would be positive and thus $q_c < q_t$. The consistent use of q_c (instead of q_t) will therefore make the estimation results more conservative (the estimated SPT N values will be smaller and the particle size of the estimated soil type will be smaller).

In CPT, the pore pressure (u) is usually measured just above the cone (Lunne *et al.*, 1997) as shown in Figure 19. In this case, q_t is expressed as:

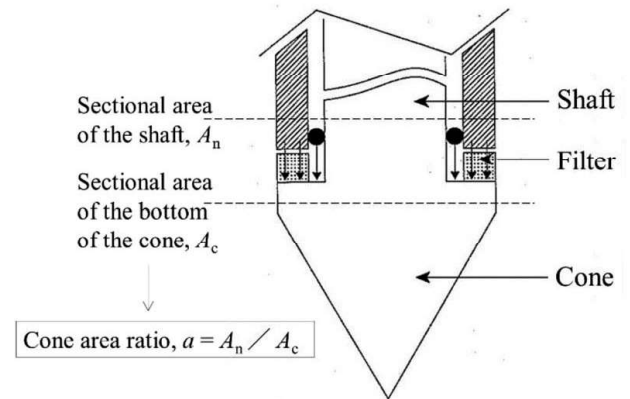


Figure 19. Typical shape of CPT cone (after JGS, 2013).

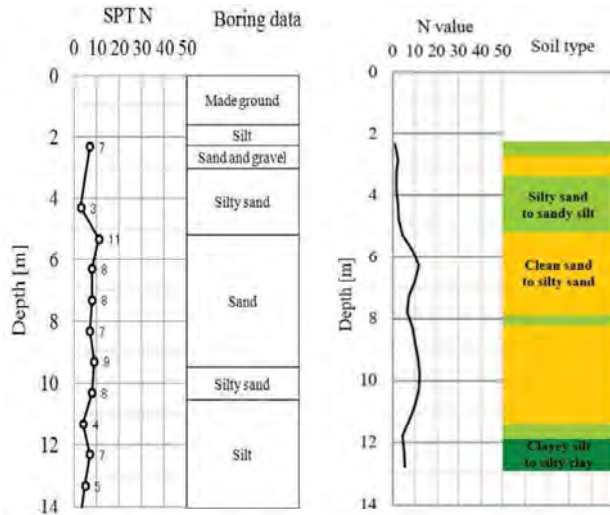
$$q_t = q_c + (1 - a) \times u = q_c + \left(1 - \frac{A_n}{A_c}\right) \times u \quad (27)$$

where a is the cone area ratio, which is the ratio of the sectional area of the shaft (A_n) to that of the widest part of the cone (A_c), as shown in Figure 19. However, JGS (2013a) recommends to obtain the value of a not based on the geometric information but by conducting an experiment in a pressure chamber.

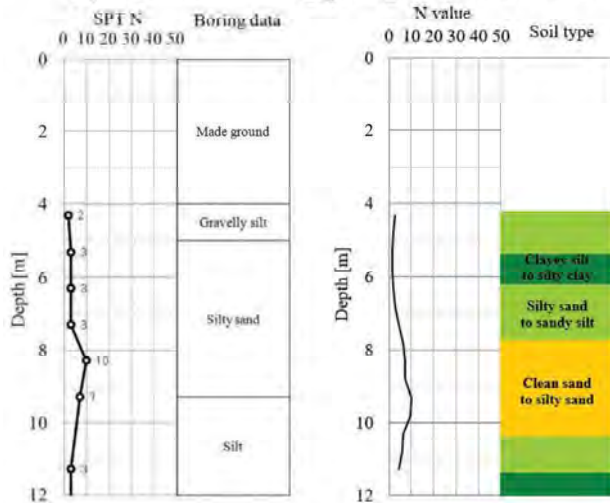
Taking one example where the generated pore pressure (u) is comparable with q_c and the “ a ” value of the cone is 0.8 (VERTEK, 2017), Equation (27) is reduced to $q_t = 1.2 q_c$.

2.5 Verification through field tests

Figure 20 shows the comparison of the SPT results with the N values and the soil types estimated from the piling data obtained during the installation of



(a) Estimation using piling data in C07-03



(b) Estimation using piling data in C09-14

Figure 20. Comparison of SPT results (left) and estimation results (right) (Closed-ended, $D_o = 318.5$ mm, $v_d = 2$ mm/s).

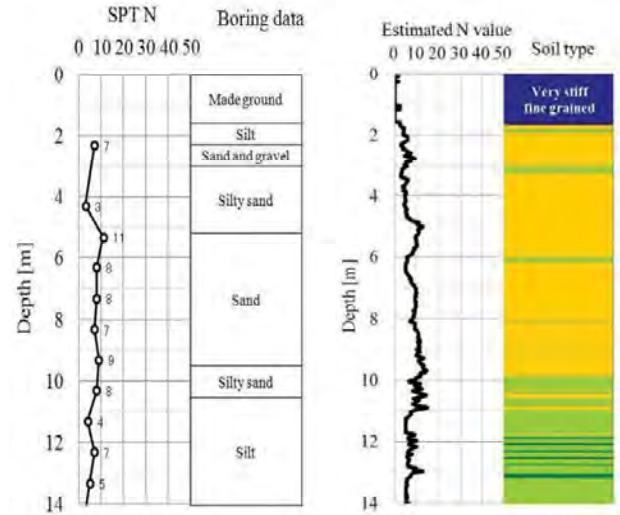


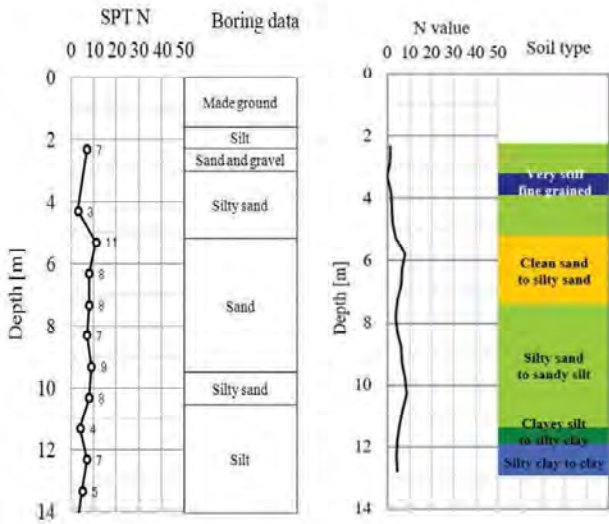
Figure 21. Comparison of N values and soil types obtained by SPT and estimated from CPT results.

a closed-ended tubular pile equipped with a base load cell ($D_o = 318.5$ mm, without surging, $v_d = 2$ mm/s). The value of Finnie factor was comparable to that of CPT so that the rate effect could be ignored. In the estimation, measured Q_b values were used instead of Equation (4). It can be confirmed that the trend of variation of the estimated N with depth agreed with the SPT results, while some of the local peak values were slightly overestimated. The differences in the depths where the local peak values were obtained would partly be because the positions of the SPT and the pile installation were different.

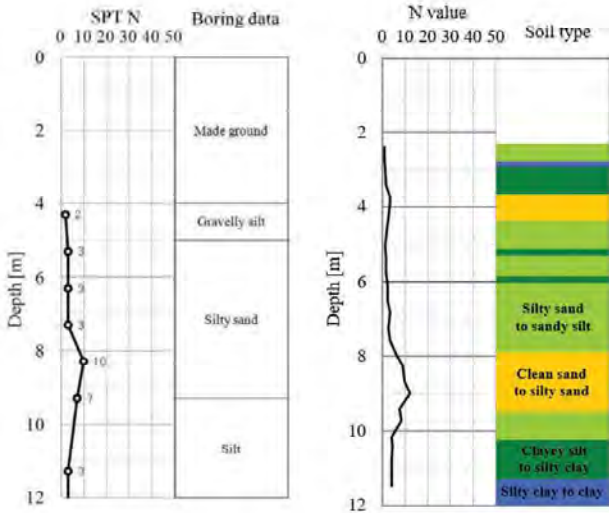
Figure 21 shows the comparison of the SPT results with the N values and the soil types estimated from CPT results. The N values were overestimated, as were in the previous case. It is suggested that this overestimating trend is the nature of the method of Equations (23) – (26). Miyasaka *et al.* (2009) conducted surveys at 36 sites in Japan and showed that the N values estimated from CPT results were greater than the N values obtained by SPT by 10% on average. One reason for this would be the influence of the energy efficiency in SPT. Equation (26) provides the N values with the energy efficiency of 60%, whereas the energy efficiency in SPT in Japan will usually be greater than 60% (JGS, 2013b), which would lead to smaller SPT N values in Japan.

Regarding the soil type, although the classification system in SPT is different from that in CPT, the soil types estimated from the piling data (Figure 20) or CPT data (Figure 21) based on the classification system in CPT roughly agreed with the SPT results.

Figure 22 shows the comparison of the SPT results with the N values and the soil types estimated from the piling data obtained during the installation of a closed-ended tubular pile equipped with a base load cell ($D_o = 318.5$ mm, without surging) at a more practical penetration rate (v_d) of 20 mm/s or 30 mm/s. In the estimation, measured Q_b values were used instead of Equation (4). As a result, the estimation results



(a) Estimation using piling data in C07-17



(b) Estimation using piling data in C11-05

Figure 22. Comparison of SPT results (left) and estimation results (right) (Closed-ended, $D_o = 318.5$ mm, $v_d = 20$ -30 mm/s).

agreed well with the SPT results. It is suggested that this would be because the overestimating trends (Figures 20 and 21) were cancelled by the rate effect.

Figure 23 shows the comparison of the SPT results with the N values and the soil types estimated from the piling data obtained during the installation of an open-ended tubular pile equipped with base earth pressure transducers ($D_o = 318.5$ mm, $D_i = 199.9$ mm, without surging, $v_d = 10$ mm/s). The length of the inner soil column (h) was obtained by a stroke sensor attached inside the pile. In the estimation, the measured base earth pressure was taken as $q_{b,closed}$, and the shaft resistance was obtained by subtracting Q_b from the head load, where Q_b was obtained by Equation (12) from q_b and IFR . As with the previous case (Figure 21), the estimation results agreed well with the SPT results.

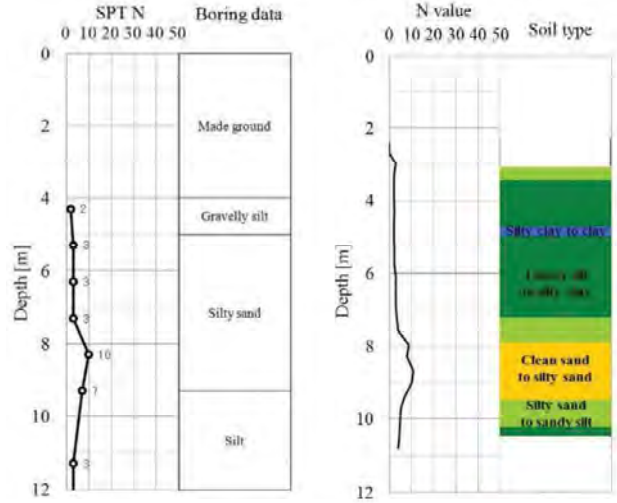


Figure 23. Comparison of SPT results (left) and estimation results (right) (C08-02: Open-ended, $D_o = 318.5$ mm, $D_i = 199.9$ mm, $v_d = 10$ mm/s).

Figure 24 shows the comparison of the SPT results with the N values and the soil types estimated from the piling data obtained during the installation of a closed-ended tubular pile ($D_o = 318.5$ mm, with surging, $v_d = 20$ mm/s). In the estimation, Q_b values were obtained by Equation (4). As a result, the estimation results agreed well with the SPT results. Looking at the figure more closely, the N values were underestimated at the depth where SPT N values were small. This will be because of the underestimating tendency of Q_b in the depth range where SPT N values are small, as discussed in Section 2.1.

Figure 25 shows the comparison of the SPT results with the N values and the soil types estimated from the piling data obtained during the installation of a sheet pile with the width of 600 mm (SP-IIIw,

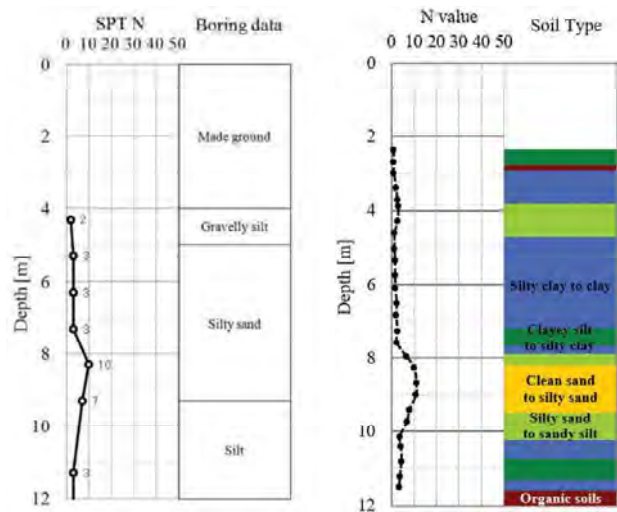


Figure 24. Comparison of SPT results (left) and estimation results (right) (C11-05: closed-ended, $D_o = 318.5$ mm, $v_d = 20$ mm/s).

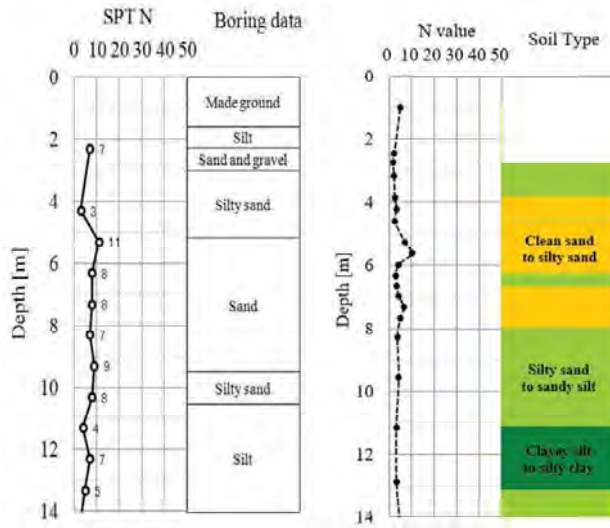


Figure 25. Comparison of SPT results (left) and estimation results (right) (J0617-05: sheet pile with the width of 600mm, $v_d = 30$ mm/s).

with surging, $v_d = 30$ mm/s). In the estimation, Q_b values were obtained by Equation (4). At the depth where local peak values of SPT N were recorded, the estimation results agreed well with the SPT results. At other depths (especially deeper than 6m), the estimation results were conservative. This will partly be because of the underestimating tendency of Q_b in the depth range where SPT N values are small, as discussed in Section 2.1. Another cause might be the assumption of IFR values being constant, although they should vary with depth in reality. If the penetration process in reality was more unplugged (having larger IFR values) than what is assumed in the estimation, the estimation results will become conservative.

Based on the above case studies, it can be said that the penetration rate and the surging stroke (downward and upward displacement in surging) do not influence the estimation results very much while the plugging condition has a significant influence on them. Especially for sheet piles, the plugging condition is assumed as being constant with depth, which can make the estimated trend of variation of N values with depth different from the actual SPT results in some cases.

Regarding the rate effect, the outer diameter of the pile is much larger than that of the CPT cone, and it could be the case that the value of the Finnie factor in press-in piling cannot be reduced to being comparable to that of CPT even if the smallest penetration rate of the press-in machine is adopted. Even so, if the values of the Finnie factor in piling and in CPT fall in between 0.1 and 30, the rate effect will be negligibly small (Bolton *et al.*, 2013). If the Finnie factor values are outside of this range, considering that the Standard Press-in is usually adopted in soft soils that might be expected to be contractile (rather than dilatant), and that the value of Finnie factor

in piling is greater than that in CPT, the unit base resistance in piling will become smaller than the tip stress in CPT, and consequently the estimation results will become conservative.

3 ESTIMATION FROM PILING DATA OBTAINED IN PRESS-IN WITH AUGERING

In Press-in with Augering, a sheet pile is installed by a static jacking force with the aid of an augering device consisting of an auger head, auger screw and casing. The similarity in the augering process and the drilling of rocks has been taken into account to estimate the subsurface information from the piling data in Press-in with Augering (Ishihara *et al.*, 2015a). The outline of the flow of estimation is shown in Figure 26.

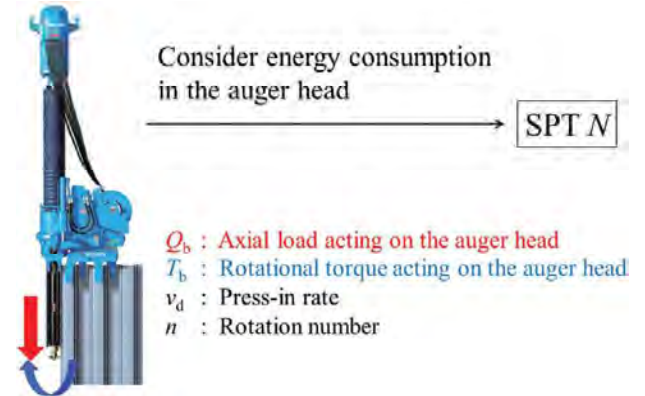


Figure 26. Flow of estimation in Press-in with Augering.

3.1 Estimation methods

In the field of rock drilling, it is known that the parameter T/d_c , where T is the effective rotational torque and d_c is the depth of cut, will be proportional to the unconfined compressive strength of a rock (Nishimatsu, 1972; Fujimoto *et al.*, 2005). Fukui *et al.* (1996) pointed out that the parameter $T/(d_c)^\gamma$ has a better correlation with the strength of the rock than T/d_c , where γ is a constant. Assuming that the similar relationship exists for the ground other than rocks, and that the unconfined compressive strength of the ground is linearly correlated with its SPT N value as was found for clays with SPT N being in between 10 and 100 (JGS, 2013c), the parameter $T/(d_c)^\gamma$ in Press-in with Augering is expected to linearly correlates with SPT N . It follows that the SPT N is estimated by:

$$N = A \times \frac{T}{\left(\frac{v_d}{n}\right)^\gamma} \quad (28)$$

where A is a constant, v_d is the downward velocity of the pile and n is the rotational revolution of the auger.

On the other hand, there is a technique called MWD (Measurement While Drilling) in the field of drilling, which estimate the hardness of the ground from the energy required for drilling it. In this technique, the SPT N is obtained by the following equation (JGS, 2004):

$$N = C_n \times \left(Q_b + \frac{2 \times \pi \times n \times T}{\nu_d} \right) \quad (29)$$

where C_n is a constant. Considering the similarity of the process of drilling to which MWD is applied and that of augering in Press-in with Augering, it is expected that this equation can be applied to Press-in with Augering by adjusting the value of C_n .

For a reliable estimation, the constants in Equations (28) and (29) should be obtained by the back-analysis based on the sets of SPT results and the piling data, so that the estimated N values agree with the SPT results.

As explained in Section 1.3, the converted N value will be adopted for hard grounds with SPT N exceeding 50 in this paper. It has to be noted that the reliability of the converted N value is limited and several methods of correction have been proposed (SN-EC, 2004). The higher the values of the converted N , the lower the reliability of the converted N would be. Considering this, it would be desirable to conduct the back-analysis of the parameters in Equations (28) and (29) based on the database of the piling data and the SPT results that are obtained in the ground where the converted N values are smaller than a certain value.

3.2 Verification through case studies

In this section, the estimated N values will be compared with the SPT results, based on the data obtained in piling construction sites. In the estimation, the values of the constants (A , γ and C_n) were obtained by the back-analysis based on the database with the converted N values smaller than 100. The values of the constants were common in all the cases. The press-in piling data were obtained during the pre-augering process using a standard type of the auger head, which has 450 mm outer diameter and 3 wings as shown in Figure 27.

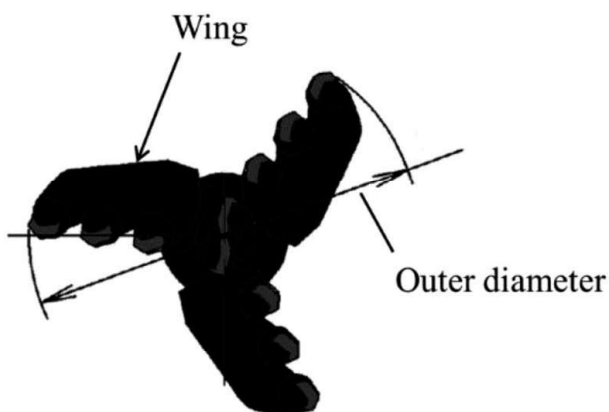


Figure 27. Standard type of auger head.

Figures 28 – 31 shows the comparison of the N values obtained by SPT and those estimated from the piling data based on the two methods explained in the previous section. In the both estimation methods, the trends of variation of N with depth were well estimated in general. However, significant differences in the values of N were found at 2 m in P0902-02 and at 7 – 9 m and 9 – 11 m in P0916-01. Reading carefully what is written in the “commentary” column in the boring log in the SPT results, the existence of gravels or cobble stones with its diameter being larger than 80 mm was commonly confirmed at these depths, which is believed to be the cause of the difference between the estimated and investigated N values at these depths. On the other hand, the differences were also found at 6 – 7 m in P0902-02 and at 12 – 13 m in P0908-02. There is a possibility that these differences

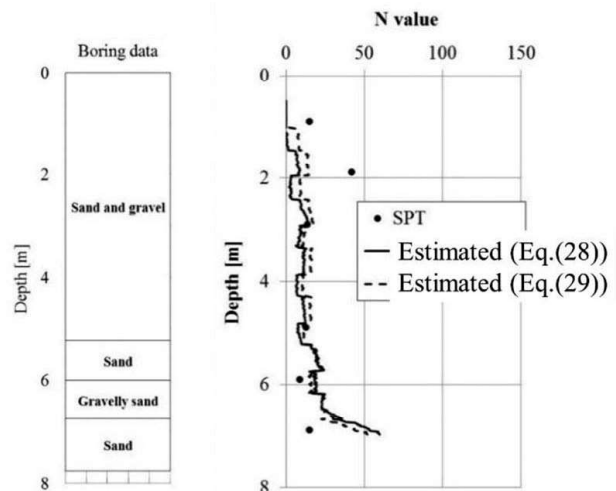


Figure 28. Comparison of SPT results and estimated N values (J0902-02).

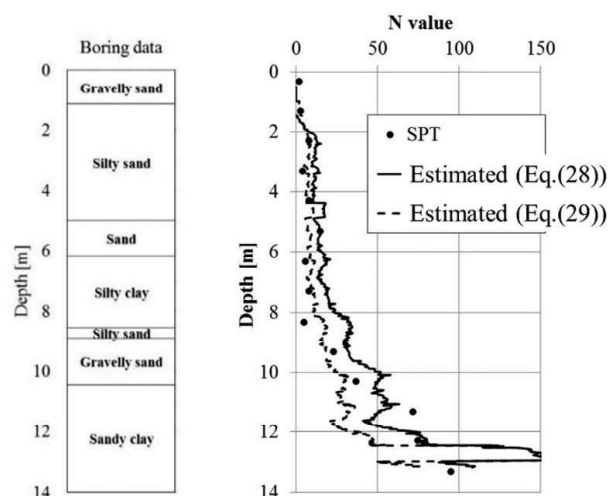


Figure 29. Comparison of SPT results and estimated N values (J0908-02).

are suggesting the existence of thin hard layers or cobbles that were not depicted by SPT which is conducted intermittently with depth (usually at every 1 m).

Comparing the estimation results obtained by the two methods, there seems to be no trend that the results obtained by one method is consistently larger or smaller than those obtained by the other. In practice, it is recommended to conduct the estimation both by the two methods and compare the results.

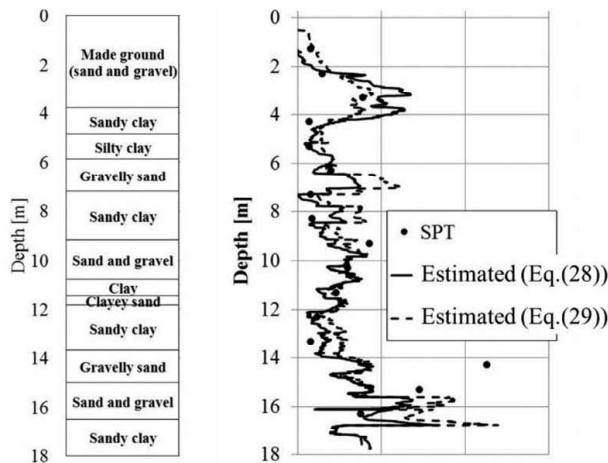


Figure 30. Comparison of SPT results and estimated N values (J0912-01).

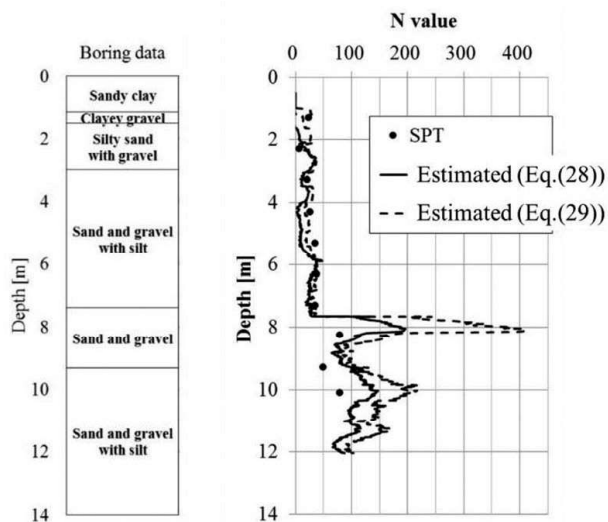


Figure 31. Comparison of SPT results and estimated N values (J0916-01).

3.3 Points to be noted

As explained in the previous section, the back-analyzed values of the constants A , γ and C_n were

obtained based on a specific type of the auger head (with 450 mm outer diameter and 3 wings), and the values cannot be directly adopted for the piling data obtained by using other types of auger heads. In the IPA-TC2 technical material, this point was reflected by restricting the use of different types of auger heads. More recently, Okada *et al.* (2018) proposed a method to allow the use of the auger heads with different diameters in the two estimation methods, by modifying the torque on the varieties of auger heads into what would be experienced on the specific type of the auger head (with 450 mm outer diameter and 3 wings) based on the model shown in Figure 32. They confirmed that their proposed method was effective in mitigating the dispersion of the estimation results that seemed to have been caused by the difference in the diameter of the auger head, as shown in Figure 33. The investigation on the applicability of this modification method has been continued using a variety of auger heads in several piling sites.

On the other hand, it should be kept in mind that the reliability of the SPT results in the hard ground would be limited. The diameter of the SPT sampler is around 50 mm, and it seems that the sampler could sometimes penetrate into the ground without hitting the gravels or cobbles that are actually contained in the ground, as reported by Ogawa *et al.* (2013). In addition, according to Mitsuhashi (1995), the cobbles usually “lie” in the ground, with their longer axis being in the horizontal plane as shown in Figure 34, and as a result the size of the cobbles written in the “commentary” column in the boring log (representing the shorter axis of the cobbles) can be smaller than one-third of the actual size of the cobbles.

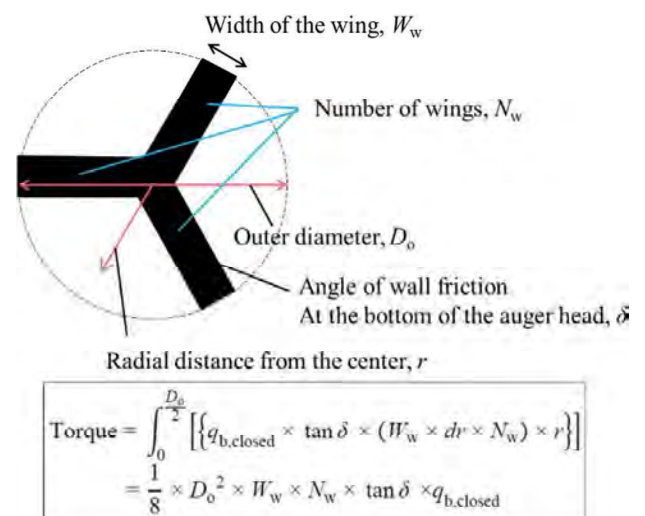


Figure 32. A model to consider different types of auger heads (after Okada *et al.*, 2018).

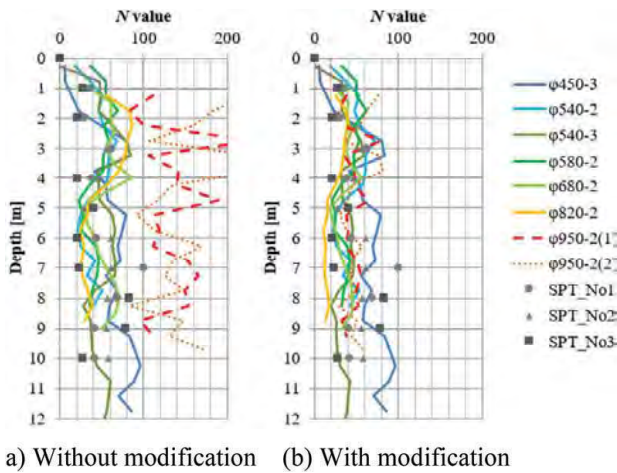


Figure 33. Comparison of N values estimated with or without the modification of torque.

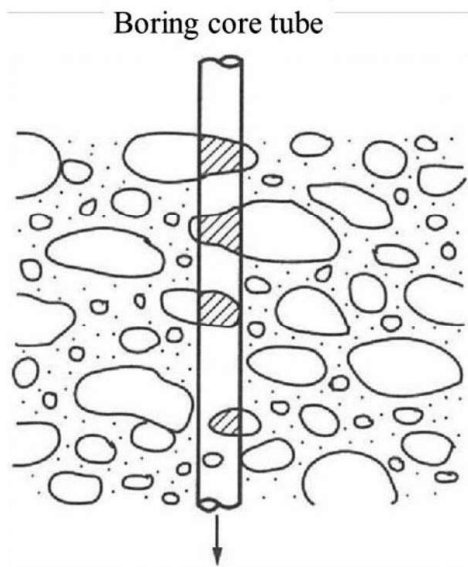


Figure 34. Boring core and cobble stones (after Mitsuhashi, 1995).

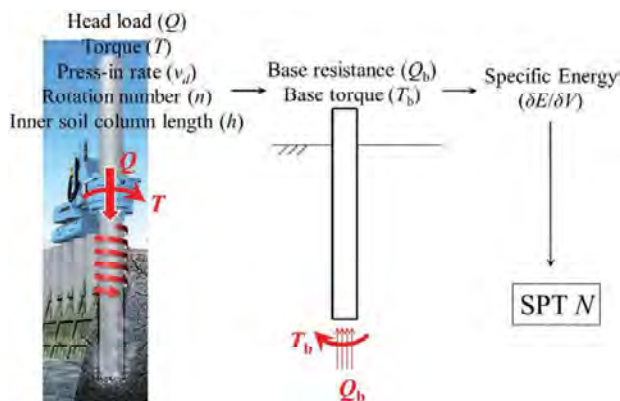


Figure 35. Flow of estimation in Rotary Cutting Press-in.

4 ESTIMATION FROM PILING DATA OBTAINED IN ROTARY CUTTING PRESS-IN

In Rotary Cutting Press-in, a tubular pile equipped with base cutting teeth is installed by the combination of vertical and rotational static jacking forces. The energy consumed for installing the pile has been considered for estimating SPT N from the piling data in Rotary Cutting Press-in, by referring to the knowledge in the field of rock drilling (Ishihara *et al.*, 2015b). The flow of estimation is outlined in Figure 35.

4.1 Estimating base resistance and base torque

4.1.1 Closed-ended piles

As discussed in Section 2.1, when estimating the subsurface in formation at the pile base, it is better to use the resistance on the pile base rather than the load applied to the pile, as the former reflects the information of the soil beneath the pile base more directly. In Rotary Cutting Press-in, the pile receives the vertical load (Q) and the torque (T) from the press-in machine, and in reaction to these it receives the base resistance (Q_b), shaft resistance (Q_s), base torque (T_b) and the shaft torque (T_s) from the ground, as shown in Figure 36 and expressed by Equations (30) and (31).

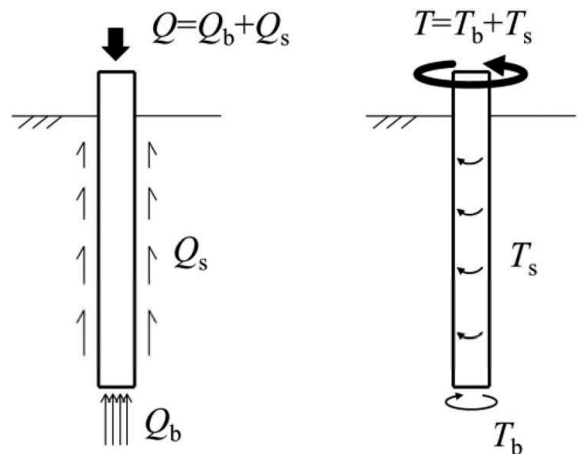


Figure 36. Forces acting on a pile during Rotary Cutting.

$$Q = Q_b + Q_s \quad (30)$$

$$T = T_b + T_s \quad (31)$$

For closed-ended piles, Q_b and T_b will be expressed as a function of the unit base resistance on the closed-ended pile ($q_{b,closed}$):

$$Q_b = \frac{\pi D_o^2}{4} \times q_{b,closed} \quad (32)$$

$$T_b = \int_0^{\frac{D_o}{2}} \{ (q_{b,closed} \times \tan \delta_{sp} \times 2\pi r \times dr) \times r \} = \frac{\tan \delta_{sp} \times \pi \times D_o^3}{12} q_{b,closed} \quad (33)$$

where r is the distance from the center of the pile in the radial direction and δ_{sp} is the frictional angle at the soil-pile interface. From these equations, $q_{b,closed}$ can be deleted to give:

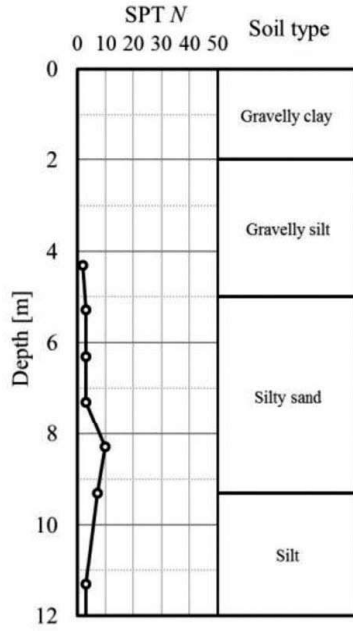
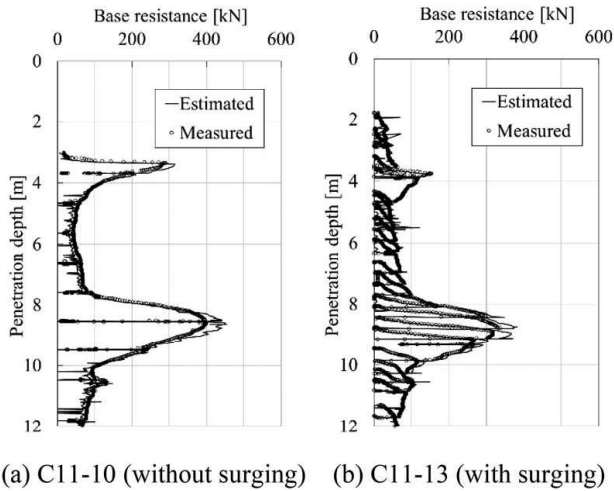


Figure 37. Site profile in C11 test series.



(a) C11-10 (without surging) (b) C11-13 (with surging)

Figure 38. Comparison of estimated and measured Q_b (Closed-ended, $D_o = 318.5\text{mm}$).

$$\frac{T_b}{Q_b} = \frac{\tan \delta_{sp}}{3} \times D_o \equiv \zeta_C \quad (34)$$

Bond (2011) showed that the frictional stress on the pile shaft (f) is shared by Q_s and T_s according to the ratio of the downward velocity (v_d) and the horizontal velocity (v_r) of the pile surface. This will be expressed as:

$$Q_s = \frac{1}{\sqrt{1+\nu^2}} \times f \times \pi D_o \times z \quad (35)$$

$$T_s = \frac{\nu}{\sqrt{1+\nu^2}} \times f \times \pi D_o \times z \times \frac{D_o}{2} \quad (36)$$

$$\nu = \frac{v_r}{v_d} \quad (37)$$

From Equations (35) and (36), f can be deleted as:

$$\frac{T_s}{Q_s} = \frac{\nu \times D_o}{2} \equiv \zeta \quad (38)$$

Combining Equations (30), (31), (34) and (38), Q_b of the closed-ended pile can be obtained by:

$$Q_b = \frac{T - \zeta \times Q}{\zeta_C - \zeta} \quad (39)$$

The validity of Equation (39) was confirmed by a series of field tests conducted in a soft alluvial soil shown in Figure 37. The pile was closed-ended and was equipped with a base load cell to measure Q_b . From the piling data (Q and T), Q_b was estimated by Equation (39), and was compared with the values measured by the load cell. As can be confirmed in Figure 38, the estimated Q_b agreed very well with the measured Q_b regardless of whether the installation was associated with surging (in Test C11-13) or not (in Test C11-10).

4.1.2 Open-ended piles

For open-ended piles, the following relationships will be supposed in the same way as were in Standard Press-in:

$$Q_b = Q_{bp} + Q_{bi} \quad (40)$$

$$Q_{bi} = \frac{\pi D_i^2}{4} \times (1 - IFR) \times q_{b,closed} \quad (41)$$

Considering that there are cutting teeth on the pile base, Q_{bp} would be expressed as:

$$Q_{bp} = t_T \times w_T \times n_T \times q_{b,closed} \quad (42)$$

where t_T and w_T are the thickness and the width of each cutting tooth and n_T is the number of the cutting teeth. In the same way as Q_b , the base torque (T_b) will be expressed as:

$$T = T_{bp} + T_{bi} \quad (43)$$

where T_{bp} and T_{bi} are respectively the torque on the pile base annulus and at the bottom of the soil column inside the pile, that arise as a reaction from the soil beneath the pile base. Assuming that a slip plane is created at the pile base, T_{bi} could be written as:

$$T_{bi} = \int_0^{D_i} \{ (1 - IFR) \times q_{b,closed} \times \tan\phi \times 2\pi r \times dr \times r \} \quad (44)$$

where ϕ is the internal friction angle of the soil around the pile base. On the other hand, assuming that a uniform stress of $q_{b,closed}$ acts both on the vertical and the horizontal planes in each cutting tooth as shown in Figure 39, T_{bp} will be expressed as:

$$T_{bp} = t_T \times d_c \times n_T \times q_{b,closed} \times \frac{D_o + D_i}{4} \quad (45)$$

$$d_c = \min\left(h_T, \frac{\pi \times (D_o + D_i)}{2 \times n_T \times \nu}\right) \quad (46)$$

where d_c is the depth of cut and h_T is the height of the cutting tooth. If IFR and $q_{b,closed}$ are independent of r , Equations (40) – (46) can be combined to give:

$$\frac{T_b}{Q_b} = \frac{3\pi t_T (D_o + D_i)^2 + (1 - IFR) \times \tan\phi \times 2\pi \nu D_{in}^3}{24\nu n_T t_T w_T + (1 - IFR) \times 6\pi \nu D_{in}^2} \equiv \zeta_{O,T} \quad (47)$$

On the other hand, the relationship between Q_s and T_s would be comparable with that for closed-ended piles, as expressed by Equation (38). Combining Equations (30), (31), (38) and (47), Q_b of the open-ended pile can be obtained by:

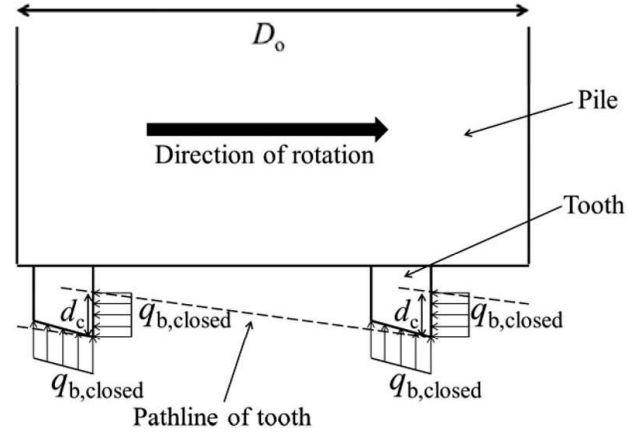


Figure 39. Assumption of the resistance on the cutting tooth.

$$Q_b = \frac{T - \zeta \times Q}{\zeta_{O,T} - \zeta} \quad (48)$$

4.2 Estimating SPT N

When a penetrating material penetrates into the ground by an incremental depth of δz , the soil beneath the base of the penetrating material will receive an incremental energy of δE and will deform by a volume of δV . In the field of rock drilling, the index $\delta E / \delta V$ is called as the Specific Energy (SE), and has been widely used to represent the performance of the drilling machines (Teale, 1965; Hughes, 1972).

According to Hughes (1972) and Li & Itakura (2012), SE in rock drilling and the unconfined compressive strength of the rock are linearly correlated. Expanding this knowledge to assume that SE required for a penetrating material to penetrate into the ground has a linear relationship with the strength of the ground, it would follow that the SE required in Rotary Cutting Press-in and the SE required for an SPT sampler to penetrate into the ground are linearly correlated, which would be written as:

$$\frac{Q_b \times \delta z + 2 \times \pi \times n \times \delta t \times T_b}{A_{b,eff} \times \delta z} = \chi \times \frac{m_w \times g \times h_w \times e \times N}{a_{b,eff} \times \delta z^*_{SPT}} \quad (49)$$

where the left side is the SE in Rotary Cutting Press-in and the fractional part in the right side is the SE in SPT. n is the revolution number, t is the time, m_w and h_w are the mass and the drop height of the weight, g is

the gravitational acceleration, e is the energy efficiency in SPT, $a_{b,eff}$ is the effective base area of the SPT sampler and δz^*_{SPT} is the reference incremental penetration depth of the sampler ($= 0.3$ m). χ is the parameter to represent the piling efficiency in terms of the energy consumption. The value of χ will become greater than unity when unnecessary energy is consumed in the piling process. This could happen when the pile is excessively extracted, inducing a drop of soils around the pile base into the cavity created by the extraction and the subsequent increase in Q_b . Another case where the energy is unnecessarily consumed could be encountered in a multilayered ground. If a high revolution number required for a pile to penetrate through hard layers is maintained in soft layers where the pile can penetrate without rotation, the energy associated with the rotation will be excessive in the soft layers.

From Equation (49), the estimated SPT N can be obtained by:

$$N = \frac{a_{b,eff} \times \delta z^*_{SPT} \times (Q_b \times \delta z + 2\pi n \times \delta t \times T_b)}{\chi \times e \times m_w g h_w \times A_{b,eff} \times \delta z} \quad (50)$$

In Rotary Cutting Press-in, the installation is often associated with surging (repeated penetration and extraction) in order to reduce the resistance and smoothen the piling process. As a machine setting, the motion of surging is displacement-controlled. If the values of Q or T exceed certain values, it will be conducted in a load-controlled manner. This is because it is necessary to maintain the values of Q and T sufficiently smaller than the reaction obtained from the pull-out resistance of the previously installed piles, the weight of the press-in machine and so on, for a smooth piling process.

Table 4. Specification of piles.

	D_o [mm]	D_i [mm]	t_T n_T [mm]	w_T [mm]	h_T [mm]
J1001	800	776	6 40	65	80
C12	800	776	4 40	65	200
J1404	1000	976	6 40	65	200
J1501	1000	976	6 40	65	200

If the installation is associated with surging, the pile base passes a certain depth several times. The energy consumption in the surging process would be considered by integrating Equation (50) as:

$$N = \frac{a_{b,eff} \delta z^*_{SPT}}{\chi e m_w g h_w} \int \left(\frac{Q_b \delta z + 2\pi n \delta t T_b}{A_{b,eff} \delta z} dz \right) \quad (51)$$

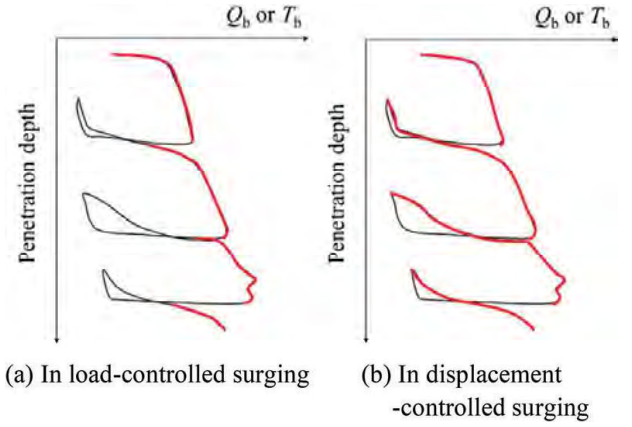


Figure 40. Data used for the integration in Equation (51).

Through the application of the piling data obtained in Site N1 (mentioned later), it was confirmed that a better agreement in the N values estimated by Equation (51) and those obtained by SPT was found if the integration in Equation (51) was conducted using the data recorded in the penetration into the fresh ground (Figure 40a) when the surging motion was controlled by displacement, while it was better to use the data recorded when the pile was moving downward (Figure 40b) if the surging was conducted in a load-controlled manner.

4.3 Verification through field tests

Field tests were conducted in two different sites to confirm the validity of the estimation method for open-ended piles with base teeth. The specification of the piles and the press-in conditions are summarized in Tables 4 and 5, where v_u is the upward velocity of the pile, f_w is the flowrate of water injected in the pile base, l_u is the upward displacement in each cycle of surging, and Q_{UL} and T_{UL} are the manually-set upper-limit values of Q and T respectively. The symbol “-” means that no specific values were set (i.e. arbitrary values were adopted).

The site profile in the first site (Site A) is shown in Figure 41. It is multilayered and inhomogeneous in plan in the depth range from 3 m to 8 m below the ground surface. The positional relationship of the SPT and the pile installation is shown in Figure 42.

In the estimation, χ was assumed as unity, and PLR (Plug Length Ratio, defined by Equation (52)) (Xu *et al.*, 2005) was adopted in place of IFR .

$$PLR = \frac{h_{EOI}}{z_{EOI}} \quad (52)$$

Here, h_{EOI} and z_{EOI} are the length of the soil column inside the pile and the penetration depth of the pile at the end of installation. It is believed that the use of

Table 5. Press-in conditions.

	v_d	v_u	v_r	Q_{UL}	T_{UL}	l_u	f_w	Site
	[mm/s]	[mm/s]	[mm/s]	[kN]	[kNm]	[mm]	[l/min.]	
J1001-1	12-16	22	240	400	-	60	30	A
J1001-4	12	22	240	500	-	40	30	A
C12-21	8	6	150	600	-	40	90	N1
C12-22	8	18	110	600	-	40	90	N1
J1404-5	10	30	340	600	500	40	60	N1
J1501-3	-	-	-	600	-	20-80	60	N1

PLR instead of IFR did not deteriorate the validity of the estimation in Site A, as the pile installation proceeded in a fully unplugged manner ($IFR = PLR = 1$).

Figure 43 shows the N values estimated from two sets of piling data (jacking force Q , torque T , time t , penetration depth z and the length of the inner soil column h) obtained in Site A. The estimated N values agreed well with the SPT results, showing relatively small values (between 10 and 15) in $0\text{ m} < z < 10\text{ m}$ and a steep increase to more than 30 in $10\text{ m} < z < 12\text{ m}$. On the other hand, some differences were found in the two estimated values in $3\text{ m} < z < 4\text{ m}$. These differences would be due to the inhomogeneity of the ground, judging from the differences in the four SPT results in Figure 41.

The site profile in the second site (Site N1) is shown in Figure 44. It consists of a sand layer and a sand and gravel layer. The sand and gravel layer seems dense and have large N values (exceeding 50 at several depths). The positional relationship of the SPT and the pile installation is shown in Figure 45.

Figure 46 shows the N values estimated from three sets of piling data obtained in Site N1. In the estimation, χ was taken as unity and PLR was used instead of IFR. The estimated N values gradually increased with depth in $z < 8\text{ m}$, and exceeded 50 at several depths in $10\text{ m} < z < 12\text{ m}$. These trends agree with the SPT results as a whole. Significant overestimations were found at 8.5 m in C12-22 and at 7 m in J1404-5. These would be because large l_u values (around 500mm in both cases) were adopted around these depths to cope with the deterioration of the piling efficiency caused by the phenomenon of plugging or the sudden increase in the frictional stress called “water binding” (Stevens, 2015). On the other hand, some overestimations were confirmed in $8\text{ m} < z < 12\text{ m}$. This will mainly be because PLR was adopted instead of IFR in the estimation. This point will be further discussed in the next paragraph.

It has been understood that the transition of the plugging condition during the pile penetration can be explained by the equilibrium of forces that act on the

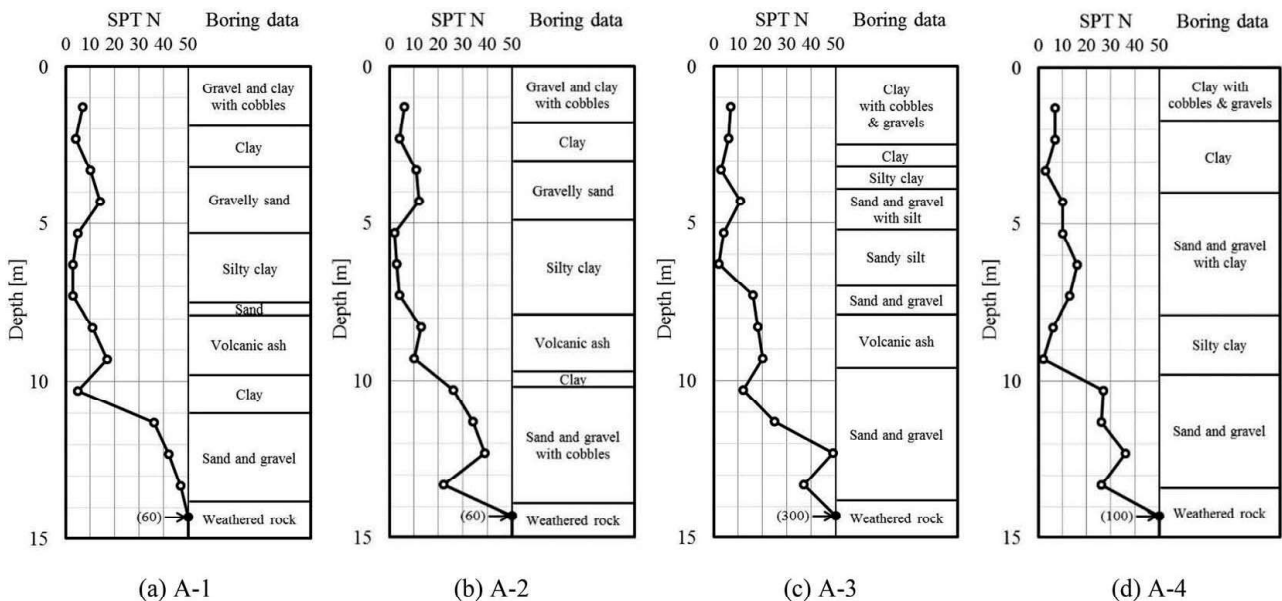


Figure 41. SPT results in Site A.

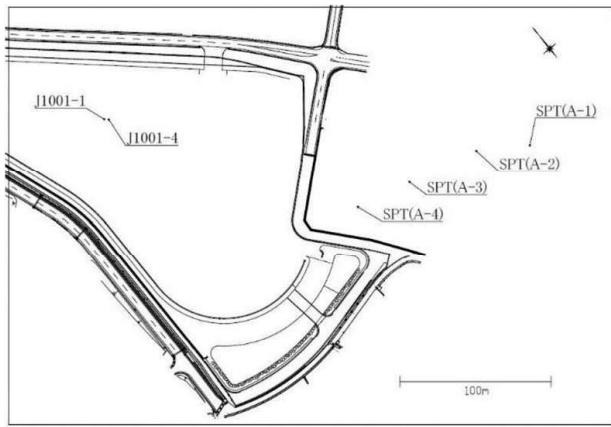


Figure 42. Positional relationship of SPT and pile installation in Site A.

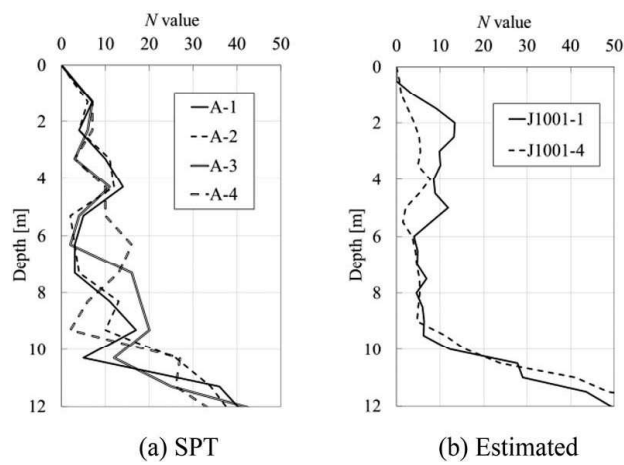


Figure 43. Comparison of N values obtained by SPT and estimated from piling data in Site A.

soil column inside the pile (White *et al.*, 2000; Okada & Ishihara, 2012). The pile will become plugged where N values decrease with depth, because the push-up stress on the bottom of the soil column will decrease with depth. At such depths, PLR becomes larger (closer to 1) than IFR , leading to smaller $A_{b,eff}$ based on Equation (12). As a result, N values estimated by Equation (51) becomes larger. Figure 47 shows the comparison of the N values estimated by using PLR or IFR , and the N values obtained by SPT. Note that IFR values were obtained as the average over the depth range of 0.5 m, to cope with the insufficient frequency of measuring h relative to the frequency of surging, and the N values were estimated by the following equation:

$$N = \frac{a_{b,eff} \delta z^*_{SPT} \delta z^* (Q_b \delta z + 2\pi n \delta t T_b) dz}{\chi e m_w g h_w A_{b,eff} \delta z^*} \quad (53)$$

where δz^* is the reference value of the incremental penetration depth (= 0.5 m). In $10\text{ m} < z < 12\text{ m}$, N values were significantly overestimated if PLR was used, but the overestimating trend was mitigated if IFR was used. As can be confirmed in Figure 48, the penetration became almost fully plugged (i.e. IFR was nearly zero) in deeper than 10 m. However, although the significant overestimating trend in $z > 10\text{ m}$ was mitigated if IFR was used, the variation of N with depth became too eminent. This might have been caused by the use of IFR values averaged over 0.5 m.

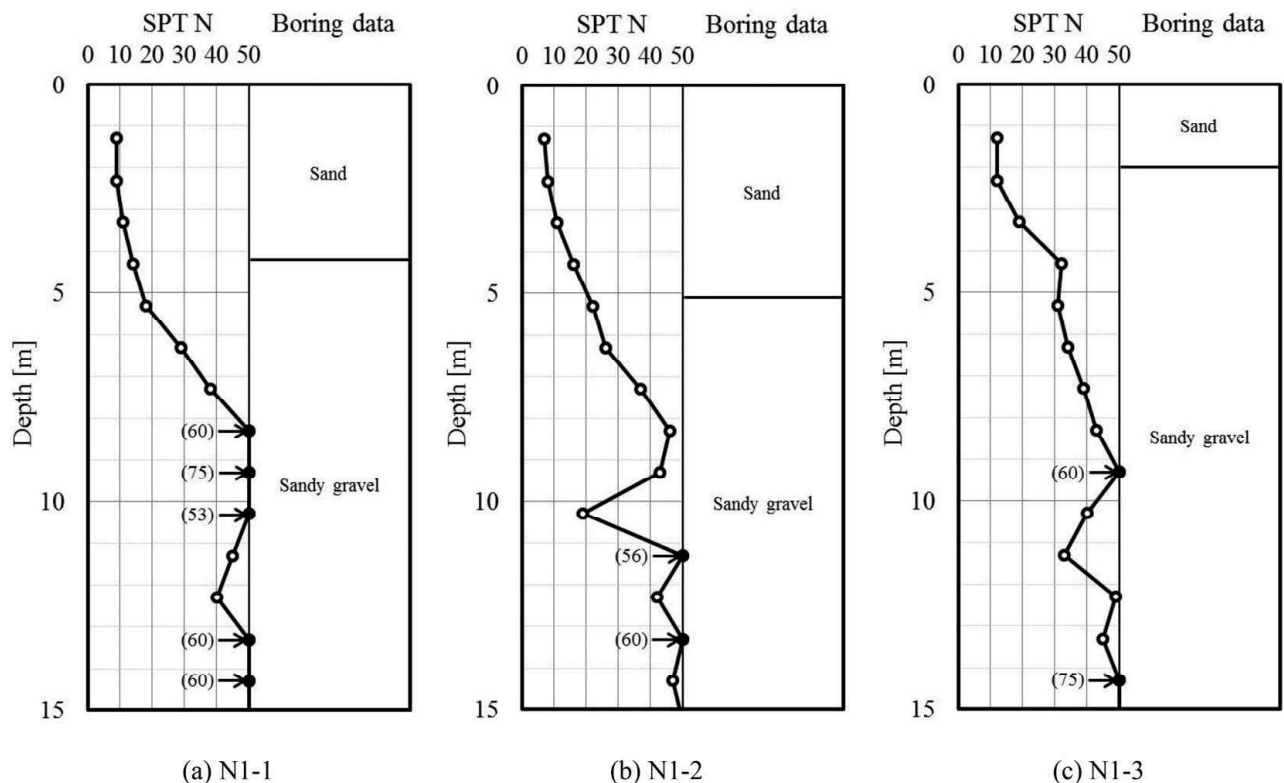


Figure 44. SPT results in Site N1.

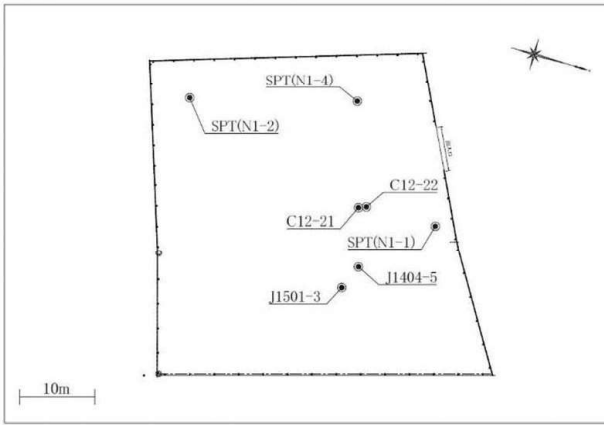


Figure 45. Positional relationship of SPT and pile installation in Site N1.

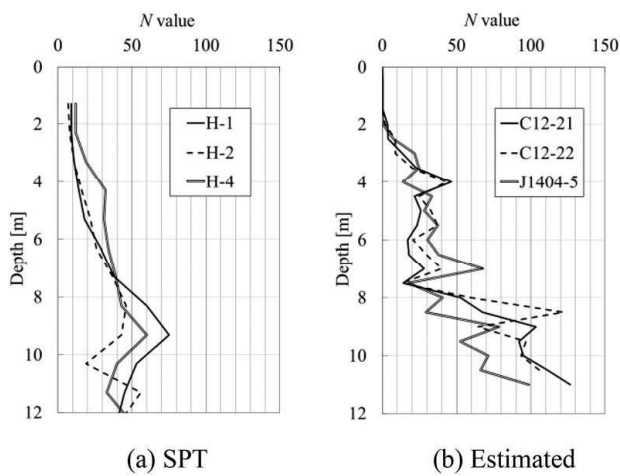


Figure 46. Comparison of N values obtained by SPT and estimated from piling data in Site N1.

From these case studies, it can be said that the penetration and the downward and upward displacement in surging have small influence on the estimation results, while the plugging condition (values of IFR or PLR) influences significantly. If the plugging condition varies with depth to some extent, the estimation results based on PLR will become less reliable, and it is recommended to use IFR obtained by a continuous measurement of the length of the inner soil column (h). In addition, the sampling rate (frequency of the measurement) of h should be sufficiently high, so that the IFR values in each cycle of surging can be used to conduct the integration in Equation (51).

5 POSSIBLE UTILIZATION OF THE ESTIMATION METHODS AND REMAINING ISSUES

5.1 Possible utilization of the estimation methods

As discussed in the previous sections, the subsurface information estimated by the methods in this paper

agreed as a whole with the information obtained by the subsurface investigation techniques, but showed some disagreement under certain conditions. Such disagreements would sometimes be caused by the difference in the mechanical conditions such as the size and the shape of the pile, the CPT cone or the SPT sampler, and sometimes by the difference in the geological conditions due to the inhomogeneity of the ground. On the other hand, the subsurface investigations conducted several times in one site can yield results that are not consistent with each other. Considering these points, it would be recommended at the present stage that the subsurface information estimated by the methods in this paper be limitedly used as a reference when managing the termination of piling or judging the alteration of the penetration techniques, as exemplified below:

- (1) Contractors confirm the bearing stratum by grasping the variation of the estimated N with depth, and assure an adequate embedment depth of the pile.
- (2) Contractors adequately alter the press-in conditions required for the operation of the press-in machine and attempt to improve the piling efficiency, based on the estimated subsurface information.
- (3) When encountering the unexpected ground conditions, contractors put together the estimated subsurface information and present them to the owners, and propose the alteration of the construction plan such as the re-selection of the installation assistance.

If the estimated information significantly disagrees with the subsurface investigation results and its validity needs to be carefully investigated, it is recommended to conduct additional subsurface investigations by the other methods. If the

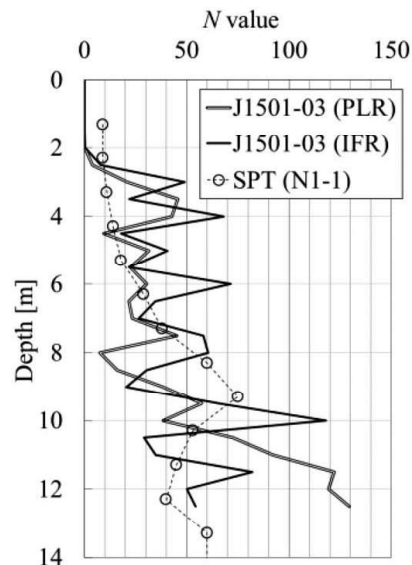


Figure 47. Differences in N values estimated by using PLR or IFR .

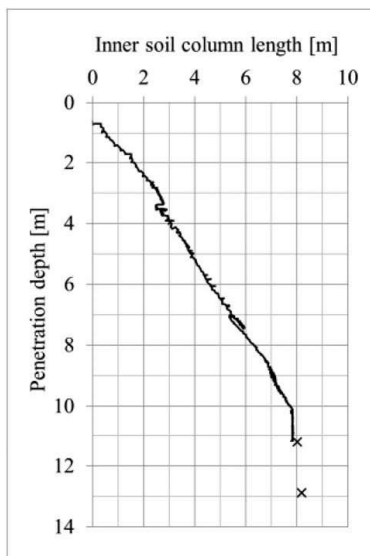


Figure 48. Variation of the inner soil column length with depth in J1501-03.

cause for the disagreement is expected to be the existence of gravels, cobbles or underground obstacles, it is desirable to avoid the use of SPT as an additional investigation method, considering the limitation of its applicability to such conditions as discussed in Section 3.3. The most reliable method would be the trial digging, where a backhoe could be used for a shallow excavation and a set of a casing tube and a hammer grab could be effective if the target depth is deep. The large-diameter core tube sampling (Watanabe *et al.*, 2006) might be another option. On the other hand, the ground-penetrating radar could be a choice if its difficulty in distinguishing cobbles from cavities (Kimura *et al.*, 2000) are overcome. The surface-wave method could also be adopted if its resolution is improved.

In Rotary Cutting Press-in, the reliability of the estimation results will be deteriorated if the plugging condition significantly varies with depth and the measurement of the inner soil column length is omitted or conducted with an insufficient sampling rate. It is recommended to measure the inner soil length with a sufficient sampling rate to grasp its variation during surging and conduct the integration in Equation (51).

5.2 Remaining issues

For Standard Press-in, the following points would be effective in improving the validity of the estimation methods:

- (1) It is necessary to refine the method of considering the effective base area or the plugging condition of the sheet piles. Although the equivalent tubular pile was introduced in this paper, the actual direction of the shear stress on the sheet pile is different from that on the tubular pile. In addition, the

plugging condition was assumed to be constant for each type of sheet pile in this paper, but it will vary with depth depending on the state of soils around the sheet pile. One option to better reflect the actual situation might be to consider the phenomenon as the increase in the shaft resistance as a result of the arching action to increase the horizontal stress, as discussed by Taenaka (2013).

- (2) It is necessary to consider the effect of the penetration rate on the unit base resistance quantitatively. In this paper, the Finnie factor was used to find the conditions where the rate effect can be ignored or deemed to make the estimation results conservative. If the variation of the unit base resistance is expressed as a function of the Finnie factor, the rate effect can be more directly considered. In addition, in using the Finnie factor, an adequate definition of D_o for sheet piles and the effect of surging on the drainage condition have to be investigated.
- (3) It is necessary to investigate the regionality of the correlation between CPT and SPT. Methods to correlate them that were used in this paper were developed based on the database obtained in the North American Continent, and as discussed in Section 2.5, applying the methods to the CPT data obtained in Japan led to slightly overestimating trends of N values.
- (4) It is necessary to investigate the scale effect, especially for large-diameter piles. In this paper, it was supposed that the scale effect is constant regardless of the pile diameter, according to White & Bolton (2005). However, the database was limited to piles having the diameter of about 1000 mm or smaller, and for larger piles it still remains possible that the unit base resistance becomes smaller as the pile diameter becomes larger, as have been widely understood. If so, applying the estimation methods in this paper to large-diameter piles will make the estimation results conservative.

For Press-in with Water Jetting, no methods have been developed. It is necessary to collect the piling data before establishing an estimation method.

In Press-in with Augering, the following points would be effective in improving the validity or expand the applicability of the estimation methods:

- (1) It is necessary to continue collecting the data sets of SPT results and the piling data and conduct the back-analysis of the parameters to increase the versatility of the parameters. It is desirable that the positions of the SPT and the press-in piling are as close as possible.
- (2) It is necessary to investigate the values of the parameters for hard grounds including rocks, to expand the applicability of the estimation methods.

In Rotary Cutting Press-in, the following points would be effective in improving the validity of the estimation methods:

- (1) It is necessary to further investigate the relationship between the plugging condition and the inner shaft resistance, particularly the validity of Equation (44).
- (2) It is necessary to confirm the validity of the assumption of the force acting on the cutting teeth (Equation (45)).
- (3) It is necessary to develop a device to measure the length of the inner soil column at a sufficient sampling rate without difficulty.

6 CONCLUSIONS

This paper introduced the methods of estimating the subsurface information from the data obtained in Standard Press-in, Press-in with Augering and Rotary Cutting Press-in, most of which were organized into a technical material in Japanese under the activity of IPA-TC2 in 2017. The validity of these estimation methods was assessed by conducting the field tests or collecting the data in the piling construction sites. As a result, it was confirmed that the estimation results agreed to a certain extent with the SPT results. It was also confirmed that the plugging condition influenced the estimation results significantly.

Based on the above assessment, the subsurface information estimated by the methods in this paper is recommended to be limitedly used as a reference when managing the termination of piling or judging the alteration of the penetration techniques, at this present stage. Further researches are expected to improve the validity or expand the applicability of the estimation methods.

ACKNOWLEDGEMENTS

The authors appreciate the advices and discussions on the contents in this paper, which were made by the following members of IPA-TC2 (Technical Committee on Estimation of Subsurface Information Using Press-in Data): Dr. Yoshiaki Kikuchi, Dr. Junichi Koseki, Dr. Yoshito Maeda, Dr. Tatsunori Matsumoto, Dr. Masaaki Terashi, Ms. Nanase Ogawa and Mr. Koichi Okada.

REFERENCES

- Bolton, M. D., Haigh, S. K., Shepley, P. and Burali d'Arezzo, F. 2013. Identifying ground interaction mechanisms for press-in piles. *Press-in Engineering 2013: Proceedings of 4th IPA International Workshop in Singapore*: 84–95.
- Bolton, M. D., Kitamura, A., Kusakabe, O. and Terashi, M. 2020. *New Horizons in Piling*, CRC Press: 170p.
- Bond, T. 2011. Rotary jacking of tubular piles. *M.Eng. Project Report, Cambridge University Department of Engineering*: 50p.
- Chow, F. C. 1997. Investigations into the behavior of displacement piles for offshore foundations. *Ph.D. thesis, University of London (Imperial College)*.
- Finnie, I. M. S. and Randolph, M. F. 1994. Punch-through and liquefaction-induced failure of shallow foundations on calcareous sediments. *Proceedings of International Conference on Behaviour of Offshore Structures, BOSS'94*: 217–230.
- Fujimoto, A., Takenouchi, Y., Ogura, Y., Kobayashi, S. and Haino, H. 2005. Development of rational construction method for road tunnel junctions. *JSCE Proceedings of Tunnel Engineering*, Vol. 15: 323–330. (in Japanese)
- Fukui, K., Okubo, S. and Homma, N. 1996. Estimation of rock strength with TBM cutting force and site investigation at Niken-goya tunnel. *Journal of MMIJ*, Vol. 112: 303–308. (in Japanese)
- Hashizume, Y., Uchida, K. and Kiya, Y. 2002. Construction management of bored concrete pile. *Proceedings of the 37th Japan National Conference on Geotechnical Engineering*: 1391–1392. (in Japanese)
- Hughes, H. M. 1972. Some aspects of rock machining. *International Journal of Rock Mechanics & Mining Sciences*, Vol. 9: 205–211.
- International Press-in Association (IPA). 2016. *Press-in retaining structures: a handbook, First edition 2016*: 520p.
- International Press-in Association (IPA). 2017. *Technical Material on the Use of Piling Data in the Press-in Method, I. Estimation of Subsurface Information*: 63p. (in Japanese)
- International Press-in Association (IPA). 2020. *Press-in Piling Case History Volume 1*: 198p.
- Ishihara, Y., Okada, K., Nishigawa, M., Ogawa, N., Horikawa, Y. and Kitamura, A. 2011. Estimating PPT data via CPT-based design method. *Proceedings of the 3rd IPA International Workshop in Shanghai, Press-in Engineering 2011*: 84–94.
- Ishihara, Y., Ogawa, N., Okada, K. and Kitamura, A. 2015a. Estimating subsurface information from data in press-in piling. *Proceedings of the 5th IPA International Workshop in Ho Chi Minh, Press-in Engineering 2015*: 53–67.
- Ishihara, Y., Haigh, S. and Bolton, M. D. 2015b. Estimating base resistance and N value in rotary press-in. *Soils and Foundations*, Vol. 55, No. 4: 788–797.
- Ishihara, Y. 2018. Use of press-in piling data for automatic operation of press-in machines and estimation of subsurface information. *Proceedings of the First International Conference on Press-in Engineering 2018, Kochi*: pp. 651–660.
- Jackson, A. M., White, D. J., Bolton, M. D. and Nagayama, T. 2008. Pore pressure effects in sand and silt during pile jacking. *Proceedings of the 2nd BGA International Conference on Foundations*, CD: 575–586.
- Japan Federation of Construction Contractors (JFCC) and Concrete Pile Installation Technology Association (COPITA). 2017. Methods to confirm the bearing stratum in pile construction management: 21p. (in Japanese)
- The Japanese Geotechnical Society (JGS). 2004. Other soundings. *Japanese Standards for Geotechnical and Geoenvironmental Investigation Methods*: 329–337. (in Japanese)

- The Japanese Geotechnical Society (JGS). 2013a. Electric cone penetration test. *Japanese Standards and Explanations of Geotechnical and Geoenvironmental Investigation Methods*, Vol. 1: 392. (in Japanese)
- The Japanese Geotechnical Society (JGS). 2013b. Standard penetration test. *Japanese Standards and Explanations of Geotechnical and Geoenvironmental Investigation Methods*, Vol. 1: 279–316. (in Japanese)
- The Japanese Geotechnical Society (JGS). 2013c. Standard penetration test. *Japanese Standards and Explanations of Geotechnical and Geoenvironmental Investigation Methods*, Vol. 1, p. 311. (in Japanese)
- The Japanese Geotechnical Society (JGS). 2015. Method for standard penetration test. *Geotechnical and Geoenvironmental Investigation Methods, Japanese Geotechnical Society Standards*, Vol. 1: 20p.
- Japan Press-in Association (JPA). 2017. Non-staging construction method: 9p. (in Japanese)
- Japan Road Association (JRA). 2015. *Handbook on Pile Construction*: 371p. (in Japanese)
- Jardine, R. J. and Chow, F. C. 1996. *New Design Methods for Offshore Piles, Marine Technology Directorate*: 48p.
- Jefferies, M. G. and Davies, M. P. 1993. Use of CPTu to estimate equivalent SPT N_{60} . *Geotechnical Testing Journal*, GTJODJ, Vol. 16, No. 4: 458–468.
- Kimura, M., Nakamura, H. and Abe, H. 2000. The case to have confirmed the cavity which is in the cobblestone mixture gravel bed using the underground radar. *Proceedings of the 35th Japan National Conference on Geotechnical Engineering*, Vol. 35, No. 1: 427–428. (in Japanese)
- Komurka, V. E., Wagner, A. B. and Edil, T. B. 2003. Estimating soil/pile set-up. *Wisconsin Highway Research Program 0092-00-14*, Final Report.
- Kurashina, T. 2016. Model pile penetration test on the mechanism of mobilization of base capacity of an open-ended pile. *Master's thesis, Tokyo University of Science*: 106p. (in Japanese)
- Lehane, B. M. and Gavin, K. G. 2001. Base resistance of jacked pipe piles in sand. *ASCE Journal of Geotechnical and Geoenvironmental Engineering*, Vol. 127, No. 6: 473–480.
- Lehane, B. M., Schneider, J. A. and Xu, X. 2007. CPT-based design of displacement piles in siliceous sands. *Advances in Deep Foundations*: 69–86.
- Likins, G. E. 1984. Field measurements and the pile driving analyzer. *Second International Conference on the Application of Stress Wave Theory on Piles*: 296–305.
- Li, Z. and Itakura, K. 2012. An analytical drilling model of drag bits for evaluation of rock strength. *Soils and Foundations*, Vol. 52(2): 206–227.
- Lunne, T., Robertson, P. K. and Powell, J. J. M. 1997. *Cone Penetration Testing in Geotechnical Practice*. Spon Press: 312p.
- Meyerhof, G. G. 1983. Scale effects of ultimate capacity. *ASCE Journal of Geotechnical Engineering*, Vol. 109, Issue 6: 797–806.
- Mitsuhashi, K. 1995. Know-how of reading and utilizing boring data to prevent troubles: 208p., Kindaitosho. (in Japanese)
- Nishimatsu, Y. 1972. The mechanics of rock cutting. *International Journal of Rock Mechanics and Mining Sciences & Geomechanics*, Vol. 9, Issue 2: 261–270.
- Ogawa, N., Okada, K. and Ishihara, Y. 2011. Fundamental model tests on shaft resistance during press-in and extraction of closed-ended piles. *Proceedings of the Japanese Geotechnical Society Shikoku Branch Annual Meeting*: 57–58. (in Japanese)
- Ogawa, N., Nishigawa, M. and Ishihara, Y. 2012. Estimation of soil type and N-value from data in press-in piling construction. *Testing and Design Methods for Deep Foundations, IS-Kanazawa 2012*: 597–604.
- Ogawa, N., Okada, K. and Ishihara, Y. 2013. Estimation of N value using PPT data in press-in with augering. *Proceedings of the Japanese Geotechnical Society Shikoku Branch Annual Meeting*: 97–98. (in Japanese)
- Okada, K. and Ishihara, Y. 2012. Estimating bearing capacity and jacking force for rotary jacking. *Testing and Design Methods for Deep Foundations, IS-Kanazawa 2012*: 605–614.
- Okada, K., Ogawa, N. and Ishihara, Y. 2018. Case study on estimation of ground information with the use of construction data in press-in method. *Proceedings of the First International Conference on Press-in Engineering 2018, Kochi*: 371–378.
- Rauche, F., Goble, G. G. and Likins, G. E. 1985. Dynamic determination of pile capacity. *Journal of Geotechnical Engineering*, Vol. 111, Issue 3: 367–383.
- Robertson, P. K. 1990. Soil classification using the cone penetration test. *Canadian Geotechnical Journal*, 27: 151–158.
- Stevens, G. 2015. Mechanism of water binding during press-in in sand. *M.Eng. Project Report, Cambridge University Department of Engineering*: 50p.
- Story of N value Editorial Committee (SN-EC). 2004. *Story of N Value*: 29-37, Rikoh Tosho, ISBN 978-4-5446-0697. (in Japanese)
- Taenaka, S., Otani, J., Tatsuta, M. and Nishiumi, K. 2006. Vertical bearing capacity of steel sheet piles. *Proceedings of the Sixth International Conference on Physical Modelling in Geotechnics*, Vol. 1: 881–888.
- Taenaka, S. 2013. Development and optimisation of steel piled foundations. *Ph. D. thesis, The University of Western Australia*: 289p.
- Teale, R. 1965. The concept of specific energy in rock drilling. *International Journal of Rock Mechanics & Mining Sciences*, Vol. 2: 57–73.
- VERTEK. 2017. *ConePlot for CPTSND - processing and graphing software for CPT data acquired using CPTSND or CPTDAS*: 4–5.
- Watanabe, K., Araki, K. and Endo, M. 2006. Cobble or pebble survey method. *Micro Sampling Method Research Organization*: 10p. (in Japanese) http://www.microsampling.org/download/report_2006_JSTT.pdf
- White, D. J., Sidhu, H. K., Finlay, T. C. R., Bolton, M. D. and Nagayama, T. 2000. Press-in piling: the influence of plugging on driveability. *Proceedings of the 8th International Conference of the Deep Foundations Institute*: 299–310.
- White, D. J. and Bolton, M. D. 2005. Comparing CPT and pile base resistance in sand. *Proceedings of the Institution of Civil Engineers, Geotechnical Engineering* 158: 3–14.
- White, D. J. and Deeks, A. D. 2007. Recent research into the behaviour of jacked foundation piles. *Advances in Deep Foundations*: pp. 3–26.
- White, D. J., Deeks, A. D. and Ishihara, Y. 2010. Novel piling: axial and rotary jacking. *Proceedings of the 11th International Conference on Geotechnical Challenges in Urban Regeneration, London, UK, CD*: 24p.
- Xu, X., Lehane, B. M. and Schneider, J. A. 2005. Evaluation of end-bearing capacity of open-ended piles driven in sand from CPT data. *Proceedings of the International Symposium on Frontiers in Offshore Geotechnics*: 725–731.